CHAPTER 3

PART I

Synthesis and mesomorphic properties of cholesteryl 2-fluoro-4-n-alkoxybenzoates.

3.0 Introduction:

Since the discovery of the first liquid crystalline material in 1888 [1,2], chirality and optical activity have become arguably the most important topic of research in orientationally ordered fluids. Molecular asymmetry imparts form chirality to the liquid crystal, which manifests in the form of helical ordering of the constituent molecules of the phase. Followed by the first discovery of the cholesteric phase, other helical phases like the blue phases [3,4], which have a double-twist structure and chiral Sm C* phase [5,6] were discovered and characterized. During the centenary year of the discovery of the first liquid crystal, a new intermediary, chiral state of matter, the helical Smectic-A^* (twist grain boundary smectic A) phase was discovered [7]. In this phase the molecules are arranged in layers with their long molecular axes on an average normal to the layer plane, as in the Sm A phase. This arrangement rules out the possibility of formation of helix normal to the layers. Instead, the Sm A blocks rotate so as to form helical macrostructure with the axis parallel to the layer planes. Therefore unlike the other helical phases this phase has a spiraling layer order.

This novel Sm A* (TGB_A) phase is a liquid crystal analogue of the Abrikosov phase exhibited by the type-I1 superconductors. The similarities between the nematic to Sm A transition and the normal metal to superconductor transition were first pointed out by de Gennes [8]. He predicted that for a second order nematic-Sm A transition, a defect stabilized intermediate phase could occur when the liquid crystal was subjected to bend and twist distortions. This analogy was further developed by Renn and Lubensky [9] who suggested that a similar intermediary phase which they called as the twist grain boundary phase could be formed at the N^*-Sm A transition. They proposed a theoretical model for this phase. According to them, in this phase

the formation of a helical macrostructure parallel to the layer plane would be possible by incorporating a lattice of screw dislocations into the structure of a normal Sm **A** phase. The rows of such screw dislocations in the lattice were predicted to form grain boundaries and hence this twisted Sm **A** phase was called the twist grain boundary smectic **A** phase. Subsequently, a tilted analogue of the TGB_A phase was predicted at the N* to Sm C* transition which was called the TGB_C phase. Two different modifications of this phase are possible; one where the molecules are simply inclined to the layer planes without any interlayer twist within a block, and another where they form helical structures normal to the layer planes (similar to that of a Sm C* phase) in addition to the helices formed by the screw dislocations.

The first experimental confirmation of the existence of the TGB_A phase was made by Goodby ***et al.*** [7,10] with the synthesis of 1-methylheptyl-4'-(4"-n-alkoxyphenylpropioloyloxy)biphenyl-4-carboxylates. Three homologues of this series exhibited TGB_A phase and had the following phase transitions: $I \leftrightarrow TGB_A \leftrightarrow Sm\ C^*$. X-ray diffraction and polarimetry studies have been used to verify the presence of this new phase. Subsequently a wider range of compounds and mixtures of materials that exhibit this phase have been discovered. These include propiolate systems [11-14], aliphatic substituted benzoate esters, tolanes [15-18] ***etc.*** Many of these compounds show the phase sequence predicted by Renn and Lubensky ie., $N^* \leftrightarrow TGB_A \leftrightarrow Sm\ A$. The theoretical phase diagram proposed by Renn and Lubensky is shown in figure 3.1

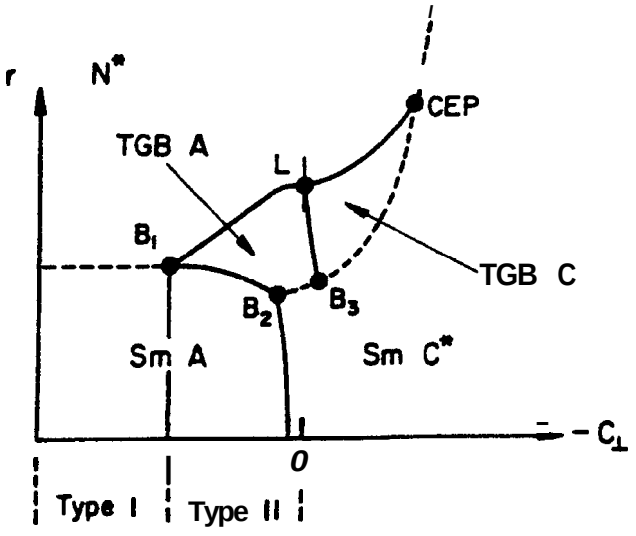

Fig 3.1 : Theoretical phase diagram of TGB_A phase proposed by Renn and Lubensky.

3.1 Factors affecting the formation and stability of TGB_A phase:

Since the discovery of the first TGB_A material, an increasing number of compounds have been investigated to obtain this phase. Molecular chirality is one of the prime factors that controls the formation and stability of the TGB_A phase. Goodby and co-workers [13] have studied the effect of size, shape and polarity of the lateral group at the chiral center on the molecular chirality. Any factor that increases the molecular chirality of the system favours the formation and stabilization of the TGB_A phase.

3.1.1 Effect of increasing the peripheral terminal chain length at the chiral center on the stability of the TGB_A phase:

Increasing the length of the terminal aliphatic chain appended to the chiral center is expected to increase the molecular chirality of the system as the chiral center will become buried in the overall structure of the molecule, thereby effectively restricting or damping the rotational freedom of the chiral center with respect to the molecular core. Slaney et ***al.*** [19] have studied this effect in homologous series of compounds in which derivatives of amino acids were used as the chiral building blocks. Consider the following two examples:

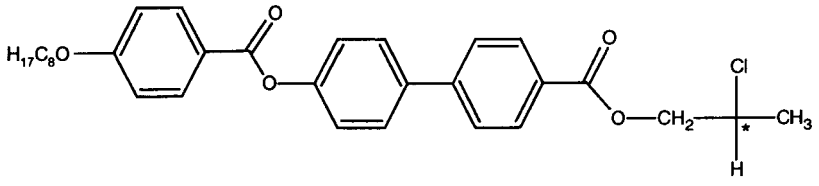

I 193.0 N^* 190.1 Sm A 72.7 Sm C^*

(3.1) [19]

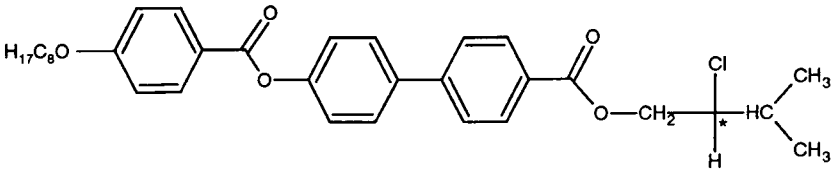

I 164.1 BPIII 163.9 BPII 163.6 BPI 160.7 N* 160.2 TGB_A 160.2 Sm A 125.5 Sm C*

(3.2) [19]

Comparison of the phase sequence and transition temperatures of compounds **3.1** and **3.2** indicates that compound **3.1** which has a short terminal chiral chain, does not exhibit TGB_A phase and instead exhibits a Sm **A** phase with a long thermal range. This is because the chiral center carrying a relatively short alkyl chain is free to rotate about the long axis of the molecule which reduces the overall molecular chirality. However in **3.2.** where there is an extension as well as branching of the terminal alkyl chain attached to the chiral moiety, TGB_A and blue phases are induced into the phase sequence.

Goodby et al. [13,14] had also made similar studies on some propiolates and found that the above effect was valid up to a certain chain length (6 C-atoms), beyond which stability of the TGB_A phase decreases. This is because increasing the chain length beyond a critical number of carbon atoms would increase the relative size (volume) of the molecular structure there by diluting the effects of chirality. The following series of compounds illustrate this effect:

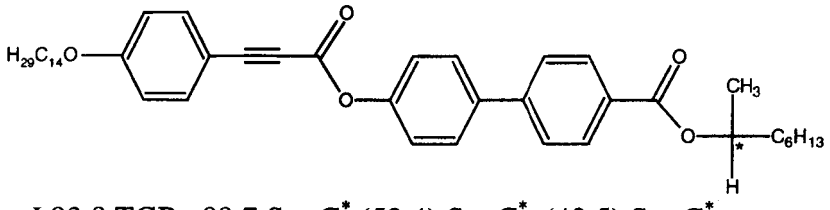

I 93.8 TGB_A 89.7 Sm C^* (53.4) Sm C^*_γ (42.5) Sm C^*_A

(3.3) [14]

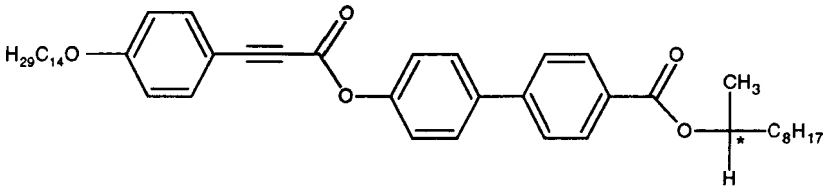

I 91.0 TGB_A 89.6 Sm C^* (38.6) Sm C^*_γ

(3.4) [14]

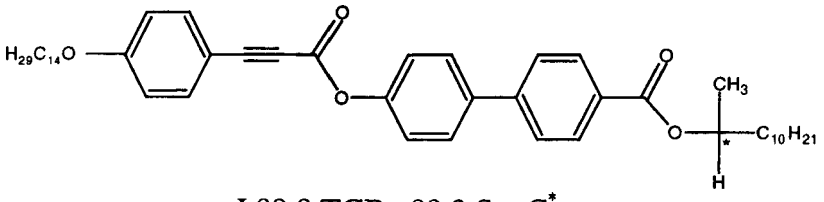

I 89.8 TGB_A 89.3 Sm C^*

(3.5) [14]

Therefore from the transition temperatures of compounds 3.3, 3.4 and 3.5 it is seen that as the number of carbon atoms in the chiral alkyl chain is increased from C_6 to C_8 to C_{10}, the stability of the TGB_A phase decreases. It is interesting to note that the stability of the tilted smectics ie., Sm c*, Sm C^*, and Sm C^*_A also follow the same trend. Infact the Sm C^*, and Sm C^*_A phases have disappeared in compound 3.5 which has ten carbon atoms in the chiral alkyl chain.

3.1.2 Effect of the number of chiral centers on the stability of the TGB_A phase:

Only a few investigations [19] have been carried out on the effect of the number of chiral centers and their absolute configuration [20] on the occurrence and stabilization of the TGB_A phase. Studies regarding this have shown that increase in the number of chiral centers result in the stabilization of the TGB_A phase. Consider the following compounds, which differ from each other by one chiral unit:

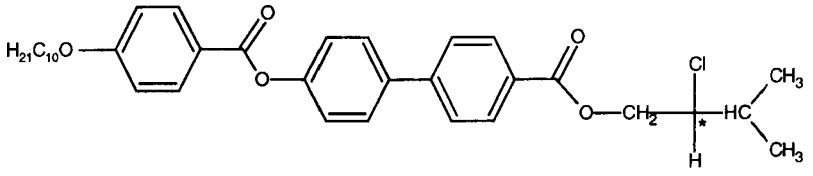

I 159.0 Sm A 125.7 Sm C^*

(3.6) [19]

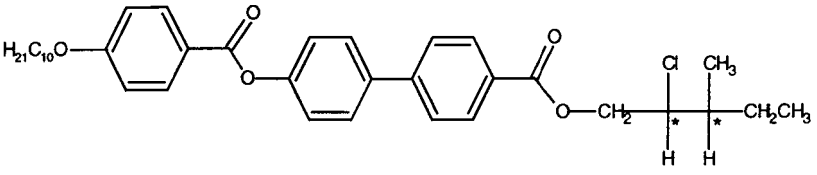

I 154.5 BPIII 154.2 BPII 153.9 BPI 151.6 N* 151.3 TGB_A 150.9 Sm A 124.7 Sm C*

(3.7) [19]

Compound 3.6, which has one chiral center, exhibits Sm A and Sm C* phases. However, when the number of chiral centers is increased to two (compound **3.7**), TGB_A and blue phases are injected into the phase sequence. Therefore it is evident from the above results that enhanced molecular chirality due to the presence of two

chiral centers in compound **3.7** as compared to compound **3.6** with a single chiral center is responsible for inducing the frustrated phase in **3.7.**

3.1.3 Effect of lateral fluoro stubstitution in the core of the mesogen on the stability of TGB_A phase:

In the last few years attempts have been made to study the influence of lateral fluoro substituents attached to the molecular core on the occurrence and stability of TGB_A phase [14,15,21]. **A** fluoro substituent is considered to be the most suitable lateral group in liquid crystal research for a variety of reasons like its small van der Waals radius [22] and fairly high polarity [23]. These properties have been frequently found to have well established effects on thermal stability [24] and other related properties [25] of the mesophase. Consider the following series of compounds:

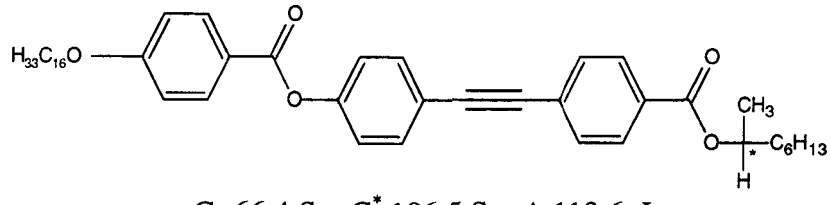

Cr 66.4 Sm C* 106.5 Sm A 113.6. I

(3.8) [21b]

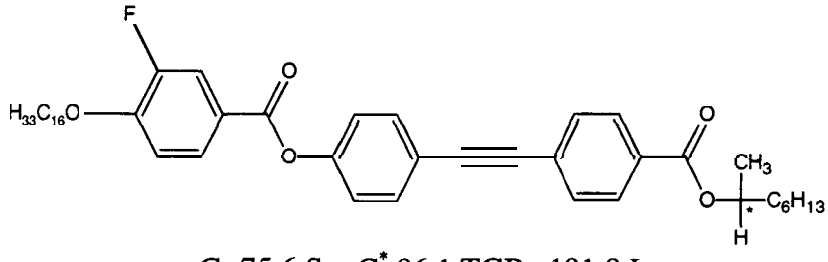

Cr 75.6 Sm C* 96.1 TGB_A 101.0 I

(3.9) [21b]

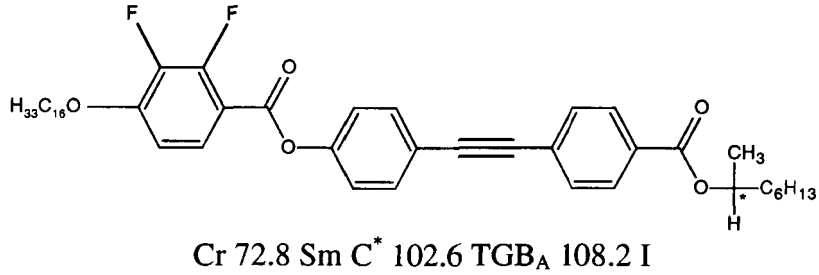

Cr 72.8 Sm C* 102.6 TGB_A 108.2 I

(3.10) [21b]

From the transition temperatures of the compounds it is seen that the unsubstituted compound (compound 3.8) has slightly higher clearing temperature than its fluorinated analogues (3.9 and 3.10) and exhibits Sm A and Sm C* phases. In compounds 3.9 and 3.10 which have lateral fluoro substituents the Sm A phase is completely eliminated and instead TGB_A phase is induced. It is interesting to note that in compound 3.10, which has a fluoro substituent towards the central molecular core in addition to the one *ortho* to the alkoxy chain, there is an enhancement in the stability of the Sm C^* phase when compared to 3.9. The reason for this has already been discussed in chapter 2. Also there is no example so far where the fluorine substitution rules out the possibility of formation of TGB_A phase.

In addition, some studies have shown that for the same alkoxy chain length, presence of a lateral fluoro substituent close to the chiral center enhances the stability of TGB_A phase. The following examples illustrate this:

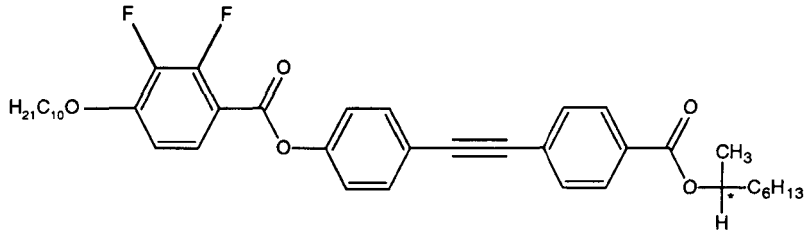

Cr73.9 Sm A 121.4 I

(3.11) [21b]

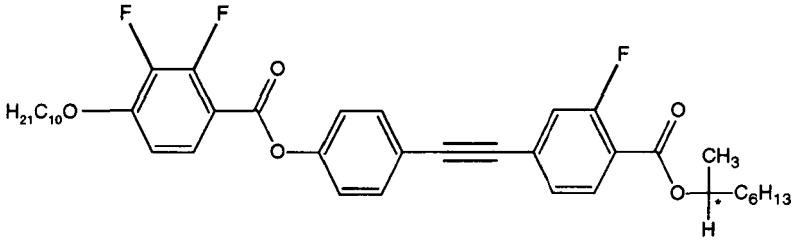

Cr 59.1 Sm C^* 98.4 TGB_A 105.8 N^* 114.5 BP 115.7 I

(3.12) [15]

Compare the structures of compounds 3.11 and 3.12. The two differ from each other by an outer-edge fluoro substituent close to the chiral center. Compound 3.11 exhibits only a Sm A phase, where as compound 3.12 shows TGB_A, Sm c*, N^* and

blue phases. The presence a lateral fluoro substituent close to the chiral center dampens the motion of the chiral group with respect to the long axis of the molecule, thereby increasing the molecular chirality and hence stabilizing the TGB_A phase.

It was believed for some time that a relatively long molecular core comprising a minimum of three aromatic rings is a prerequisite for the formation of TGB_A phase. In 1993 Nguyen ***et*** al. [26] disproved this myth by reporting the existence of this phase in homologous series of compounds composed of two phenyl rings. A survey of the literature indicates that very few compounds with cholesterol as the chiral moiety exhibit TGB_A phase [27,28,29,30]. These include dimesogenic systems, side chain liquid crystalline polymeric systems with cholesterol as the mesogenic side group and some binary mixtures having derivatives of cholesterol as one of the components.

From the discussion in sections 3.1.2 and 3.1.3, it is seen that by increasing the number of chiral centers and by having lateral fluoro substituents in a system one can enhance the chances of formation of the TGB_A phase. Our objective was to explore the possibility of obtaining TGB_A phase in compounds containing only one phenyl ring and a cholesterol moiety. To achieve this we carried out the synthesis of the following series of compounds:

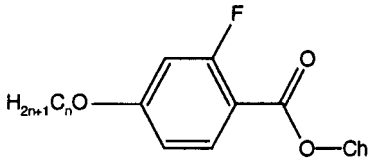

n = 12, 14, 16 **and18.**

Ch = Cholesteryl moiety.

(3.13)

We chose cholesterol as the chiral moiety for our purpose because it is a fairly long and linear molecule and has eight chiral centers. The structure of the cholesteryl unit is shown in figure 3.2.

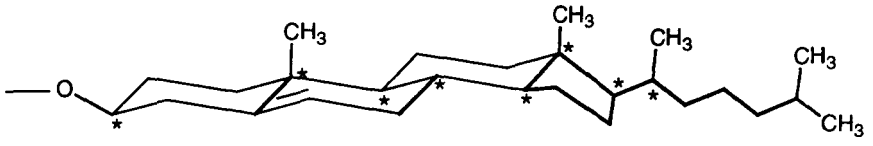

Fig 3.2 : Cholesteryl moiety.

3.2 Results and discussion:

In part I of this chapter, we describe the synthesis and mesomorphic properties of cholesteryl 2-fluoro-4-n-alkoxybenzoates. We also discuss the influence of the lateral fluoro substituent close to the chiral center on the incidence and stabilization of the TGB_A phase.

The synthesis of the compounds studied is shown schematically in figure 3.3.

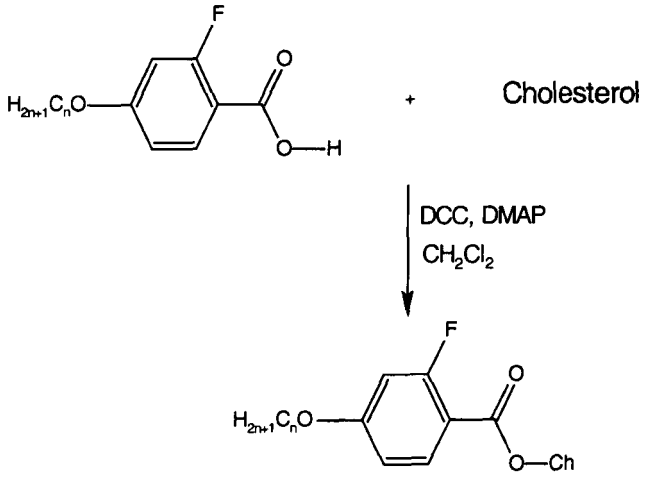

n = 12,14,16 and 18.

Fig 3.3 : Synthetic scheme for the preparation of compounds of series 3.13.

The 2-fluoro-4-n-alkoxybenzoic acids were synthesized following a procedure described by Gray, Hogg and Lacey [31]. The final esters were obtained by reacting the appropriate acids with cholesterol in the presence of a dehydrating agent such as

DCC and DMAP as a catalyst in dry dichloromethane. The cholesterol used was commercial GR-grade (ash free) precipitated from alcohol.

Different mesophases exhibited by these compounds were identified by examining thin film of a sample sandwiched between a glass slide and a cover slip under a optical polarizing microscope.

On cooling the isotropic liquid, a planar texture reflecting blue and green colours having short temperature range (0.3-0.6°C) appeared, which is characteristic of the blue phase [32]. On cooling the blue phase, both focal-conic and planar texture typical of the N* phase [32] appeared. On further reducing the temperature, multiple domains began to develop on the planar texture, which on cooling further transformed to the focal-conic texture characteristic of the Sm A phase [32]. When the Sm A phase was cooled, banded focal-conic texture typical of the Sm C^* phase [32] was formed. In order to identify the phase between the N^* and Sm A phases, the sample was examined on a homeotropically aligned cell. When the sample was heated from the homeotropically aligned Sm A phase, fine filaments began to grow in the homeotropic regions as shown in plate 3.1.

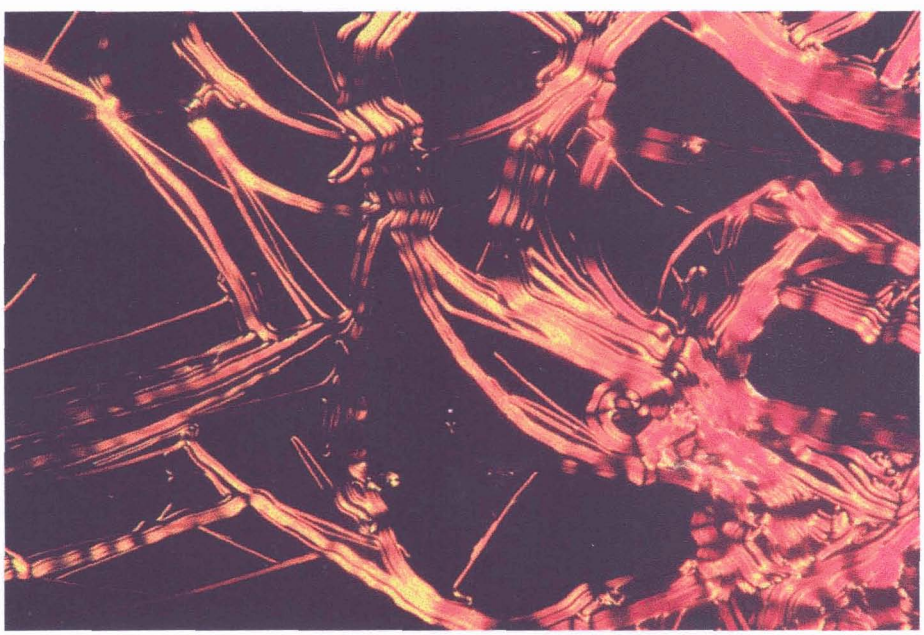

Plate 3.1 : Photomicrograph of compound 2 showing the filamentary texture of TGB_A phase originating from the homeotropic region of Sm A phase.

This texture was identical to the one observed for the TGB_A phase [10] on a homeotropically aligned cell.

As a conclusive evidence for the existence of the TGB_A phase a **Grandjean** planar texture [7] similar to that shown by the cholesteric phase was observed. This texture is best seen by taking the sample in a wedge-shaped cell treated for planar alignment. In such samples, the axis of the helix is perpendicular to the glass plates. As the **Grandjean** planar texture grows, striations (disclination lines) within the texture are seen, which possibly correspond to the integral multiples of the pitch of the helix of the phase. Plate 3.2 represents the **Grandjean** planar texture of the TGB_A phase of compound 2.

Plate 3.2 : Photomicrograph of the Grandjean planar texture of the TGB_A phase of compound 2.

The observation of the **Grandjean** planar texture also confirms the helicity in the TGB_A phase.

The phase assignments, transition temperatures and the associated enthalpy values obtained from the DSC thermograms for compounds belonging to series **3.13** are listed in table 3.1.

Table 3.1 : Transition temperatures (°C) and enthalpies (kJ mol^{-1}) for cholesteryl 2-fluoro-4-n-alkoxybenzoates.

Compound number	n	Cr		Sm C*		Sm A		TGB_A		N*		BP		I
1	12	.	118.5	-		-		-		.	194.5	.	195.0	.
			31.9								*0.05*		*0.57*	
2	14	.	105.0	.	113.5	.	147.0	.	150.5	.	185.6	.	186.0	.
			26.1		†		†		†		†		†	
3	16	.	85.0	.	97.0	.	152.5	.	154.0	.	176.9	.	177.5	.
			23.6		†		†		†		†		†	
4	18	.	94.0	(.	82.0)	.	151.5	.	152.5	.	169.8	.	170.5	.
			26.5		†		†		†		†		†	

† : The enthalpy could not be measured; ( ) : Indicates a monotropic transition.

From the table it is seen that the higher homologues of this series ie., compounds 2,3 and 4 exhibit TGB_A phase. Compound 4 which is the highest homologue of this series showed the phase sequence $BP \leftrightarrow N^* \leftrightarrow TGB_A \leftrightarrow$ Sm A $\leftrightarrow$ (Sm c*) on cooling the isotropic liquid. The Sm C* phase becomes enantiotropic in compounds 2 and 3. Compound 1 shows only N* and blue phases. Since the TGB_A phase was not seen in compound 1, other lower homologues of this series were not synthesized. The thermal range of TGB_A phase decreases on increasing the alkoxy chain length from n = 14 to 18. Compound 2 has the maximum range of TGB_A phase (3.5°C). All the compounds belonging to this series exhibited a blue phase with a short temperature range of 0.3-0.6°C.

A plot of transition temperatures as a function of the number of carbon atoms in the n-alkoxy chain is shown in figure 3.4.

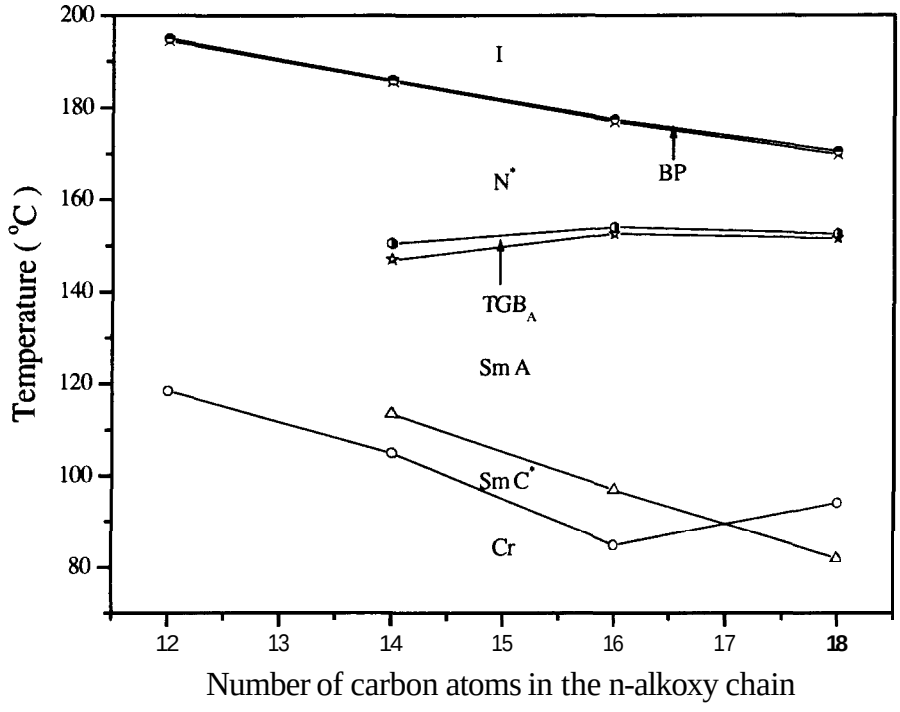

Fig 3.4 : Plot of transition temperatures *versus* the number of carbon atoms in the n-alkoxy chain.

The plot shows a smooth curve relationship for like transitions. The clearing temperatures decrease with increase in the n-alkoxy chain length. A similar trend is

seen for N* to blue phase transition temperatures also. The Sm **A** to TGB_A and TGB_A to N* transition temperatures increase initially as we increase the number of carbon atoms from **14** to **16** and then seem to level off with further increase in the alkoxy chain length from **16** to **18.** It is also interesting to note that the temperature range of the TGB_A phase decreases with increase in the alkoxy chain length.

Vill and Thiem [33] have synthesized analogous series **(3.14)** of cholesteryl 4-n-alkoxybenzoates and have examined the liquid crystalline phases exhibited by them.

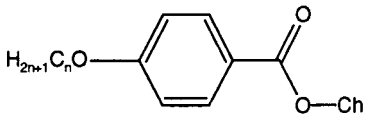

n = 1,2,3……..22.

(3.14)

According to their investigations all the compounds of this series exhibited a cholesteric phase. The homologues n = **7** to **9** showed a Sm **A** phase along with the N* phase. The higher homologues of this series ie., n = **10** to **22** exhibited a monotropic Sm C^* phase in addition to the Sm A and N* phases. The transition temperatures and the phase sequence of the homologues n = 12,14,16 and **18** belonging to this series are shown in table **3.2.**

Table 3.2 : Transition temperatures (°C) for cholesteryl 4-n-alkoxybenzoates [33]

Compound number	n	Cr	Sm C*	Sm A	N*	I
1'	**12**	**.**	**126.4 (. 84.5)**	**.**	**178.4**	**. 198.3 .**
2'	**14**	**.**	**117.0 (. 75.7)**	**.**	**176.4**	**. 188.9 .**
3'	**16**	**.**	**97.8 (. 62.8)**	**.**	**172.8**	**. 182.1 .**
4'	**18**	**.**	**105.5 (. 56.5)**	**.**	**168.3**	**. 174.5 .**

The results obtained by carrying out a comparative study between the four homologues of the series **3.14** represented in table **3.2** and the series **3.13** are summarized below.

The compounds of the two series differ from one another by the presence of a lateral fluoro substituent *ortho* to the carboxylate group close to the chiral moiety. In series 3.13, as a consequence of the lateral fluoro substituent, all the phase transition temperatures including the melting and clearing temperatures are relatively lower than those for series 3.14 (table 3.2). Compounds represented in table 3.2 show Sm A. N* and monotropic Sm C* phases where as compounds 2 to 4 in series 3.13 show a TGB_A phase in addition to the above phases. The occurrence of the TGB_A phase in series 3.13 can probably be attributed to the following two effects:

(a) Increase in the polarizability of the molecule due to the presence of a polar lateral substituent.

(b) Increase in the molecular chirality due to the restricted rotation of the chiral moiety with respect to the molecular core brought about by the lateral fluoro substituent (discussed in section 3.1.3).

Unlike series 3.14, all the compounds belonging to series 3.13 exhibited a short-range blue phase above the N* phase. Compound 1 of series 3.13 shows N* and blue phases on heating and does not exhibit Sm C* and Sm A phases like the corresponding homologue of series 3.14. It is also interesting to note that unlike the other members of the series, it does not show a TGB_A phase. From this observation it appears that the length of the alkoxy chain attached to the molecular core is also one of the important factors which governs the formation and stability of the TGB_A phase. The monotropic Sm C* phase in compounds 2' and *3'* of series 3.14 becomes enantiotropic in the corresponding homologues (2 and 3) of series 3.13.

Another example to illustrate the importance of alkoxy chain length on the occurrence of the TGB_A and other smectic phases is given below.

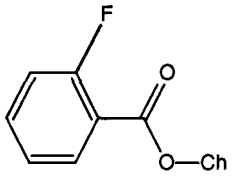

Cr 141.6 N^* 172.9 I

3.15

Compound **3.15** [34-40] exhibits only a N* phase. However by introducing appropriate lengths of the n-alkoxy chain in the 4-position of the phenyl ring one can achieve rich polymesomorphism involving the interesting frustrated helical Sm **A** phase (compounds 2,3 and 4 of series **3.13).**

Therefore, as a concluding remark it can be said that appearance of the TGB_A, Sm C* and blue phases in a single phenyl ring system having cholesterol as the chiral moiety depends on subtle changes incorporated in the molecular structure. These involve the introduction of a lateral fluoro substituent close to the chiral group and appropriate adjustment of the number of carbon atoms present in the n-alkoxy chain attached to the core.

Characterization of the final materials was carried out employing similar techniques mentioned in chapter 2. Figure 3.5 shows the DSC scan of compound 3 of series **3.13.** The heating and cooling rate was of 5°C/min. with the instrument set to maximum sensitivity in order to detect some of the weaker transitions. The TGB_A to N* and blue phase to I transitions could be resolved to some extent at slow rates, but their enthalpies could not be determined. ^{1}H nuclear magnetic resonance spectrum of compound 2 (series **3.13)** is shown in figure 3.6.

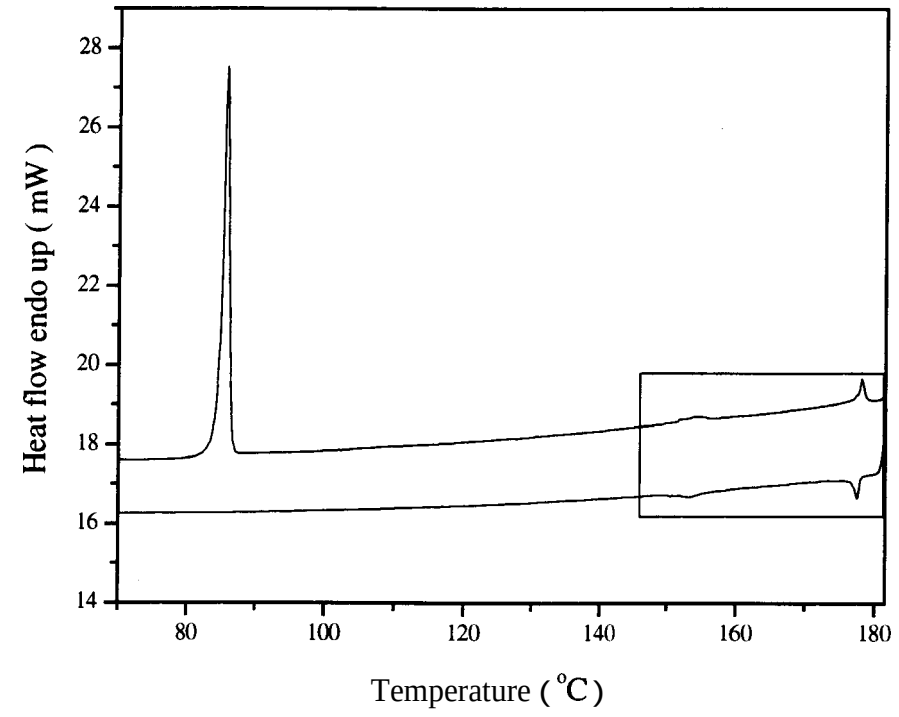

(a)

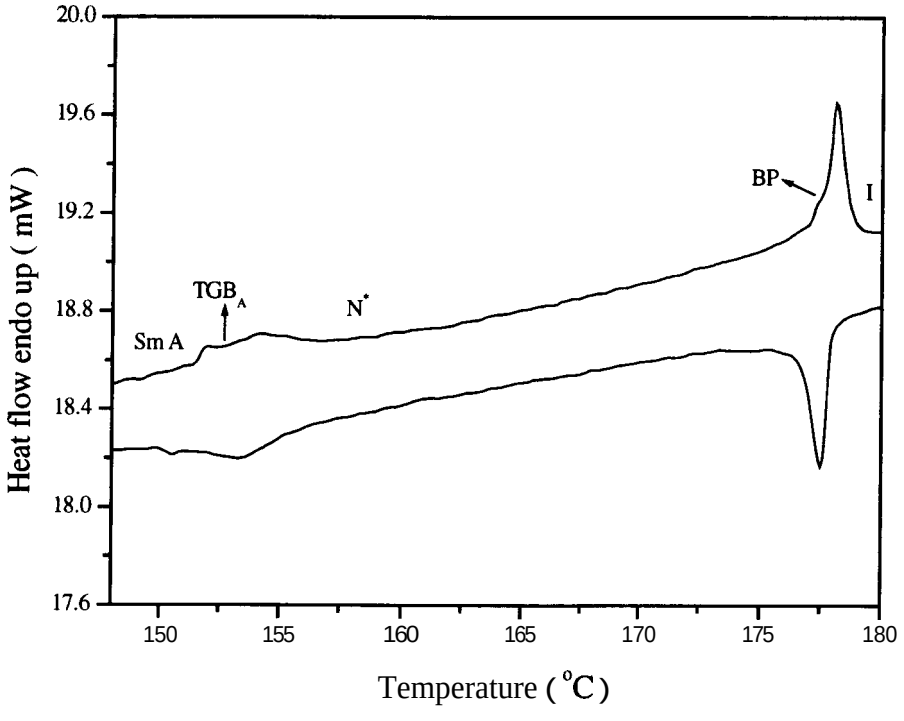

(b)

Fig 3.5 : DSC thermogram of compound 3 (series 3.13). (a) Scan at 5°C/min; (b) The enlarged view of the box shown in fig 3.4a.

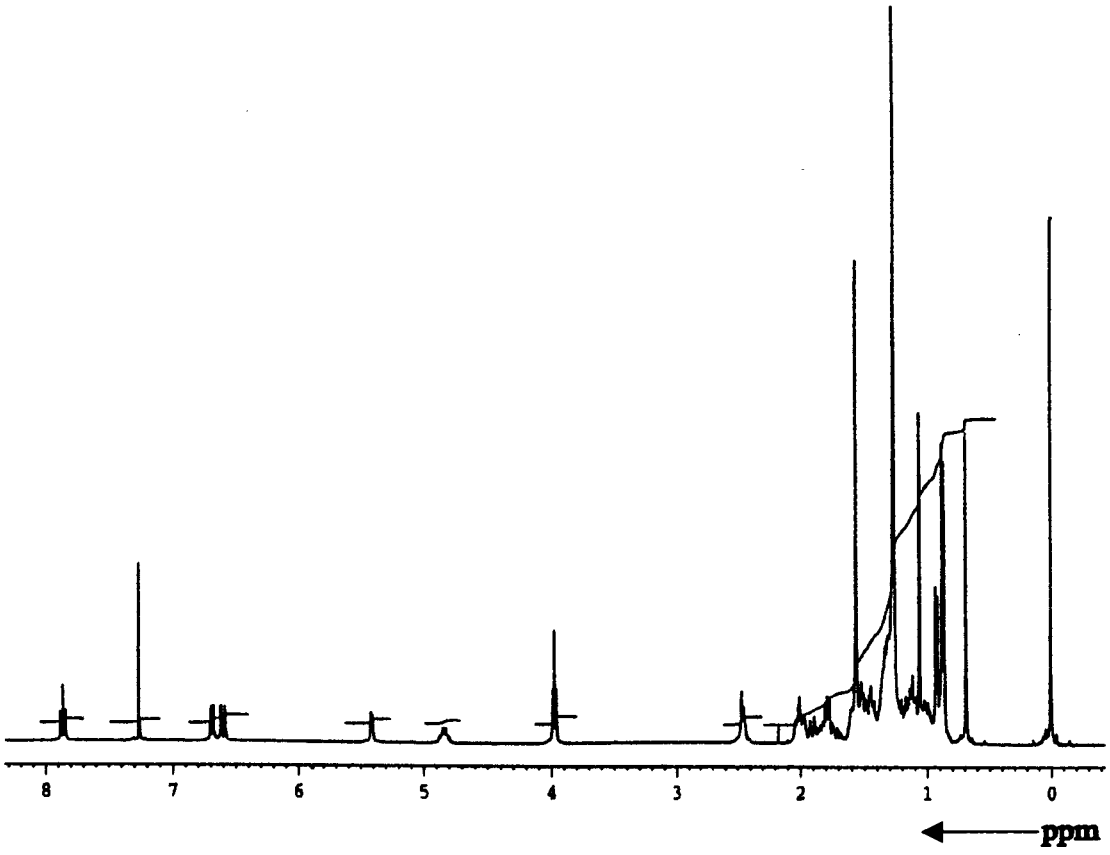

Fig 3.6 : ^{1}H Nuclear magnetic resonance spectrum of compound 2 (series 3.13).

3.3 Helical pitch measurement (p):

Helical pitch measurements on the TGB_A phase were performed by the well-known Grandjean-Cano method [41,16]. In this method the sample was taken in a small angle (≈0.5°) wedge-shaped cell treated for planar alignment, constructed by using a spacer of appropriate thickness only at one edge of the cell as shown in figure 3.7. In such samples the boundary conditions ensure that the helical axis is perpendicular to the glass plates. The local changes in the cell thickness bring about sympathetic variations in the helical pitch, thereby producing the Grandjean-plane texture (plate 3.3, section 3.2).

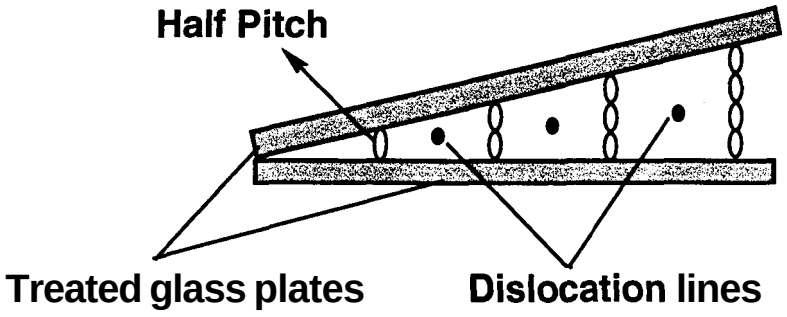

Fig 3.7 : A Schematic representation of the cholesteric/TGB structure in a wedge-shaped cell treated for planar alignment. The number of half pitches jumps by integer values across each dislocation line. The pitch gets compressed/dilated close to the dislocation lines.

It was found that across each Grandjean-Cano (GC) dislocation line the number of half pitches jumps by integer values [42]. Therefore the GC dislocation lines can be considered as edge dislocations in the cholesteric or TGB periodicity.

The sample taken in a 25μ thick wedge-shaped cell was cooled at a slow rate (0.2°C/min.) from the isotropic phase (in order to facilitate good alignment) into the cholesteric phase where an array of equidistant GC lines appeared. The pitch measurement was carried out by measuring the distance between the GC lines as a function of temperature using a graduated eye-piece, which was calibrated using a micrometer scale provided by Leitz. Before making each measurement, the sample was held for a few minutes at the required temperature till the GC lines became stationary. As the temperature was lowered the spacing between the lines increased, indicating that the pitch of the structure was increasing. The pitch value was calculated using the formula,

$$P = \frac{2yd}{l \times 10^4}$$

where y is the width of each band, d is the spacer thickness, l is the distance between the spacer and the edge of the top plate and 10^4 is the conversion factor.

Figure 3.8 shows the pitch evolution *versus* temperature in the N* and TGB_A phases for the n-tetradecyloxy homologue (compound3) of series **3.13.**

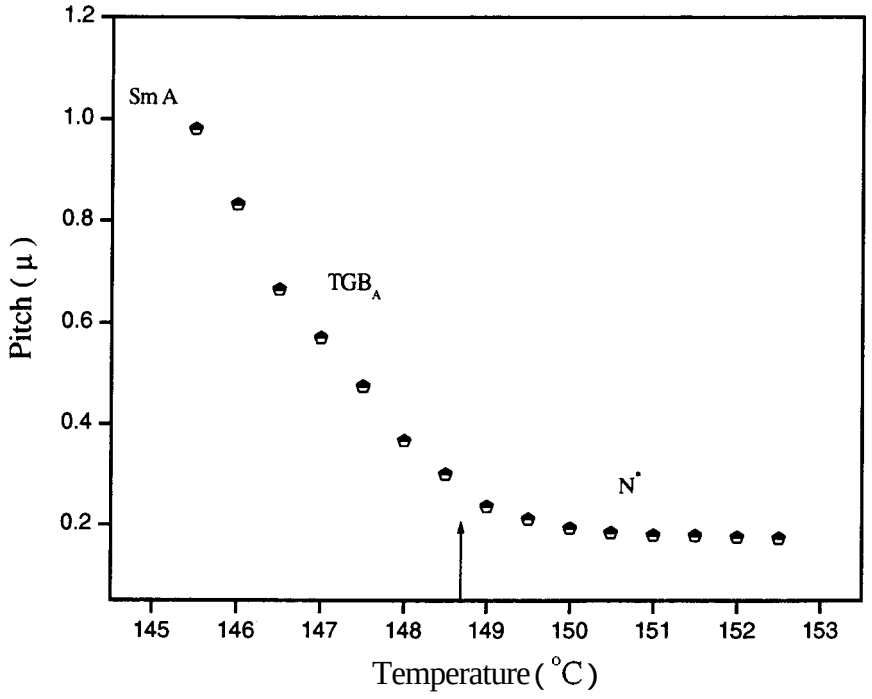

Fig 3.8 : A plot of variation of the pitch as a function of temperature in the N* and TGB_A phases.

From the plot it is evident that the variation of pitch with temperature follows a similar trend, which has been previously observed for systems exhibiting TGB_A phase [21,171. A gradual, small increase in the pitch from 0.17 to 0.19μ is observed upon cooling the sample through the N* phase. Within the TGB_A phase the pitch value rises more steeply and reaches a maximum value of 1μ at the TGB_A to Sm A transition. No discontinuity was detected in the variation of pitch at the N* to TGB_A transition.

PART II

Synthesis and mesomorphic properties of compounds exhibiting the undulated twist grain boundary smectic C*phase

3.4 Introduction:

Chirality in self-organizing media can yield a variety of novel mesophases with unique properties and structures. Under certain conditions chiral molecules can pack to give a condensed liquid crystalline phase with a helical macrostructure. One of the interesting consequences of chirality in a self-assembled media is the formation of defect stabilized frustrated structures. For example, in chiral systems, the desire for the rod-like molecules to form layered mesophase structures can be frustrated by the molecules' need to form twisted structures by virtue of their chirality, which consequently leads to the formation of a defect stabilized phase. This novel frustrated phase is called the twist grain boundary smectic A phase (TGB_A). This phase was discovered by Goodby ***et*** *al*. [10] in a highly chiral liquid crystal. The presence and to some extent the discovery of TGB phases in chiral liquid crystalline systems stems from the theoretical studies carried out by de Gennes [8]. Following the discovery of the TGB_A phase, Renn and Lubensky [43,44] extended their theoretical model to incorporate the $N^*\leftrightarrow Sm$ C* transition and predicted the existence of two other modifications namely TGB_C and TGB_{C*} phases. However only the TGB_C phase has been experimentally characterized in some detail [45,46].

Liquid crystals, being soft materials can exhibit novel geometrical structures. In the year 1997, Pramod ***et*** *al*. [47] discovered a new TGB phase whose structure was very much different from those of the other known TGB phases. They called this new phase as the undulated twist grain boundary smectic C^* ($UTGB_{C*}$) phase. This new phase was found in binary mixtures of the chiral compound 4-(2'-methylbutyl)phenyl-4'-n-octylbiphenyl-4-carboxylate and 2-cyano-4-n-heptylphenyl-4'-n-pentylbiphenyl-4-carboxylate, which have very similar lengths and molecular structures. Structures of these compounds are shown below:

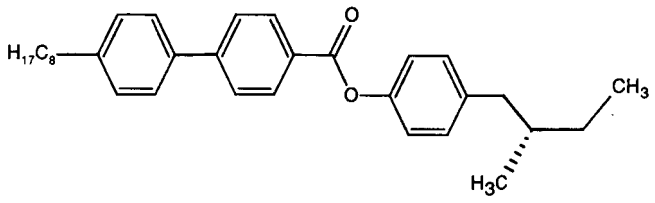

3.16

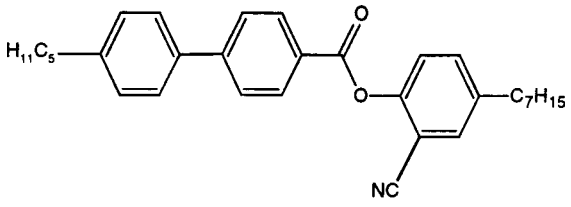

3.17

The mixture having 36 wt% of compound **3.17** exhibited this phase. Based on optical diffraction, x-ray diffraction, electrical field studies ***etc.,*** they proposed a model for this new phase. According to their model, this intermediate phase is TGB_{C^*} in nature, wherein there is a helical arrangement of tilted molecules within each Sm C^*- like blocks. In addition to this, there is a two-dimensional undulation of the Sm C^*-like blocks in the form of a square lattice. The physical origin of this phase is of greater interest because of its structural non-uniformity, with the Sm C* blocks being separated by highly defected two-dimensionally modulated grain boundaries with screw dislocations. These two parts of the structure are so different that an anisotropic interfacial energy may be invoked between the blocks. If the director configuration is Sm C^*-like, then a flat grain boundary would result in a variation in the angle made by the director with the grain boundary, along the layer normal as shown in figure 3.9a. This would cost extra energy, as the director distortion across the grain boundary will no longer be a pure twist. However, this energy can be lowered if the grain boundaries are allowed to undulate with the same periodicity as the Sm C* structure (fig 3.9b), which ensures the parallel orientation of the director to the local tangent to the grain boundary at all points. This increases the gain in chiral energy, which in turn favours the helical twist in the block.

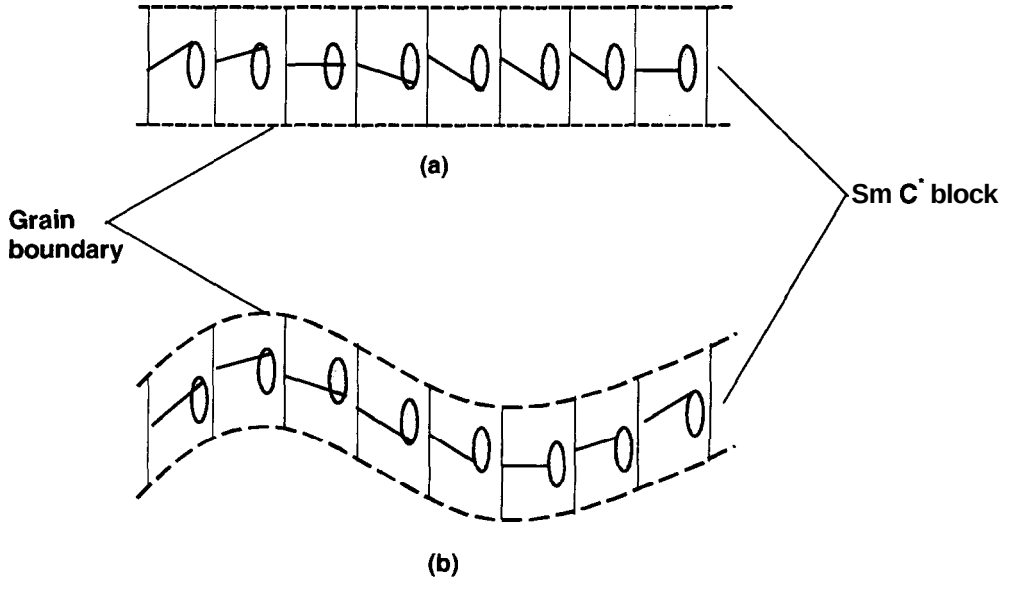

Fig 3.9 : A schematic representation of (a) a Sm C* block with flat grain boundaries and (b) a Sm C* block with undulating grain boundaries. In the former case the director makes various angles with the interface whereas in the latter case the director is everywhere parallel to the local tangent to the interface.

Experimental observations suggested that the undulation instability in the grain boundaries take place along two mutually orthogonal directions in view of the uniaxial symmetry of the TGB structure. None of the previously proposed theoretical models anticipated such a structure with the undulating grain boundaries. Since this new phase is characterized by two-dimensional undulation of the grain boundaries along with the entire structure, it is known as the undulating TGB_{C*} ($UTGB_{C*}$) phase.

Since this phase was first discovered in a mixture, the exact molecular structural requirements in a pure compound for the occurrence of this new phase were not clear. It was our desire to explore the possibility of obtaining this phase in single component systems. In view of this we carried out the synthesis of the following three series of compounds, which represent the first examples of single component systems exhibiting the novel $UTGB_{C*}$ phase.

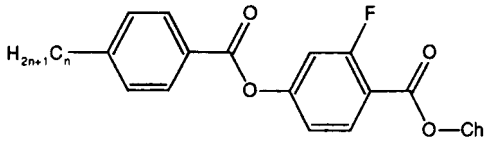

n = 8,9,10,11,12,14,16,18

3.18

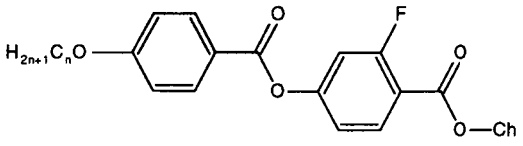

n = 9,10,11,12,14,16,18

3.19

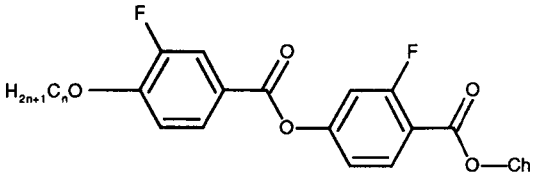

n = 7,8,9,10,11,12,14,16,18

3.20

Ch = Cholesteryl moiety (fig 3.1).

3.5 Results and discussion:

In this part the synthesis and mesomorphic properties of the compounds belonging to the series 3.18, 3.19 and 3.20 are described. A comparison of the mesomorphic properties of these compounds with those of a few other compounds with particular reference to the lateral substitution on the core and the type of chiral moiety used is also made, in order to examine the molecular structural requirements for the occurrence of this new phase.

The synthetic scheme for the homologous series of compounds under investigation is represented in figure 3.10.

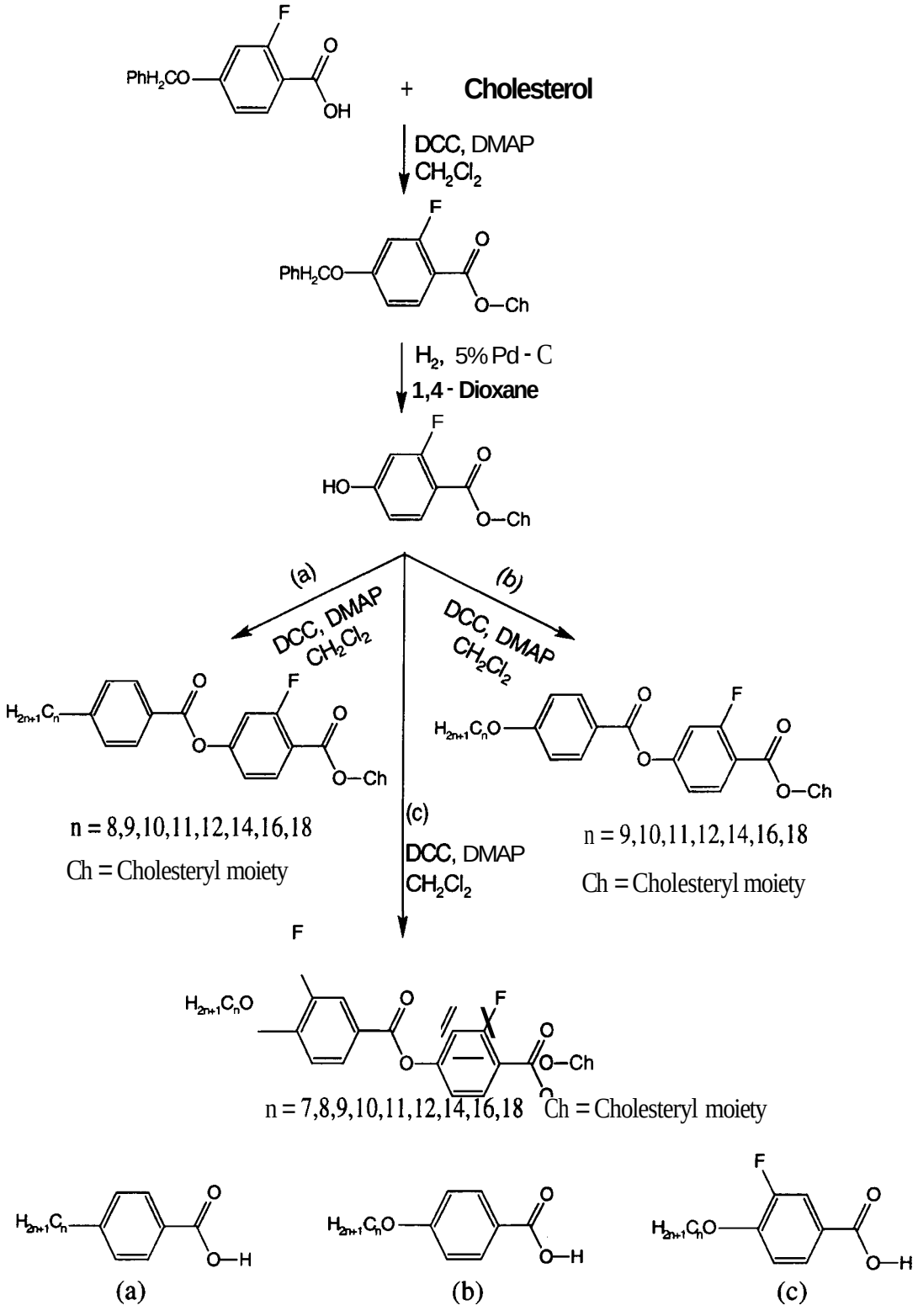

Fig 3.10 : Synthetic scheme for the preparation of compounds of series 3.18, 3.19 and 3.20.

The 4-n-alkyl/alkoxybenzoic acids were prepared following a procedure described earlier [48,49] and 3-fluoro-4-n-alkoxybenzoic acids were prepared following a procedure described in chapter 2. **2-Fluoro-4-benzyloxybenzoic** acid was prepared following a procedure described in chapter 2. Its esterification with cholesterol was accomplished in the presence of DCC, which acts as a dehydrating agent and DMAP as a catalyst. The deprotection of the phenolic group was achieved through a hydrogenolysis reaction using 5% palladium on charcoal as a catalyst. The final compounds were obtained by carrying out a similar esterification reaction of the phenol 3.32 (section 3.8) with appropriate acids. While carrying out the hydrogenolysis reaction, care was taken to prevent the reduction of the double bond in the cholesteryl moiety. The proof for the presence of the double bond in the cholesteryl moiety after the hydrogenolysis reaction is shown in the NMR spectrum (figure 3.16).

Identification of the mesophases was carried out by observing thin film of samples taken in cells of appropriate thickness, coated for both homeotropic and homogeneous alignment. Homeotropic alignment (Frank-director normal to the glass plates), was obtained by coating the glass plates with a monolayer of octadecyltriethoxysilane (ODSE) by dipping them in a dilute solution of the surfactant. The plates were then cured at 150°C for one hour. Finally the cells were constructed by using mylar strips of appropriate thickness as spacers. When the sample was heated in a homeotropically aligned cell, a pseudo-homeotropic or a schlieren texture characteristic of the Sm C* phase [32] was observed. Plate 3.3 shows the schlieren texture of the Sm C* phase.

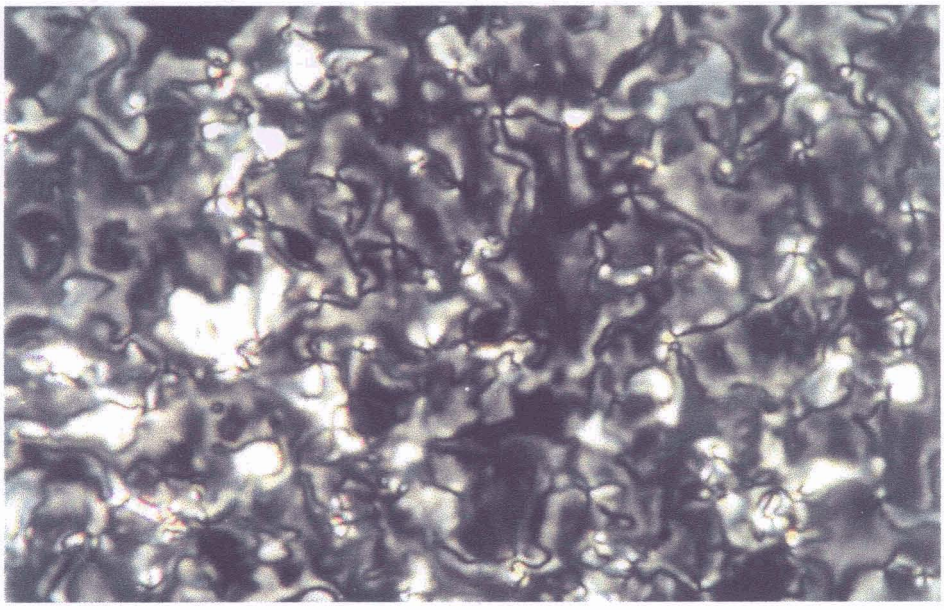

Plate 3.3 : Photomicrograph of compound 7 (series 3.18) showing the schlieren texture of the Sm C*phase (homeotropically aligned) at 154.8°C.

On heating the sample from this phase, bright corrugated filaments identical to the one observed by Pramod et al. [47] for the new $UTGB_{C^*}$ phase in the mixture, began to grow. On increasing the temperature gradually, the tips of the filaments start spiraling and they continue to grow. Plates 3.4 and 3.5 depict the corrugated filaments of the $UTGB_{C^*}$ phase.

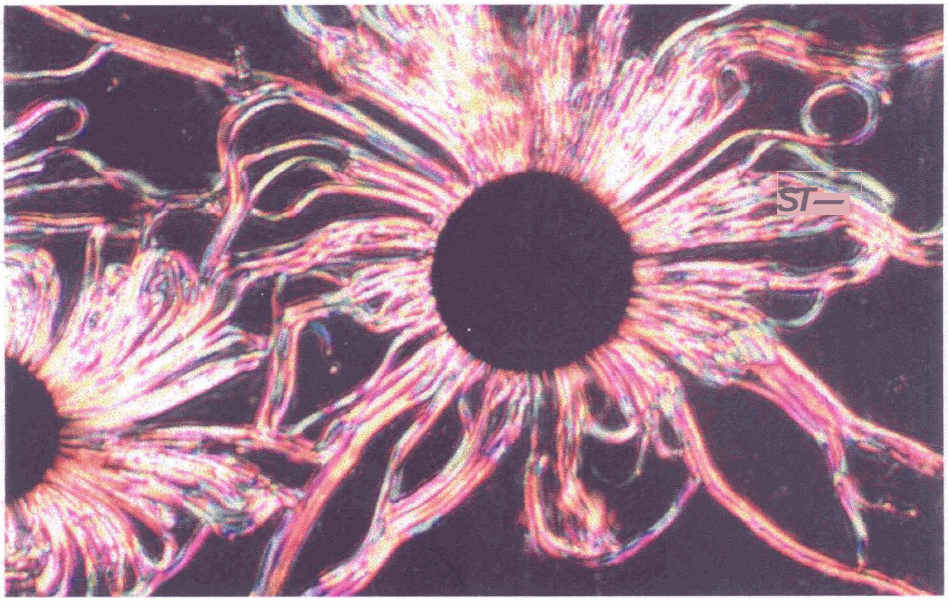

Plate 3.4 : Photomicrograph of the compound 6 (series 3.20) showing the corrugated filaments of the $UTGB_{C^*}$ (homeotropically aligned) phase at 177.3°C.

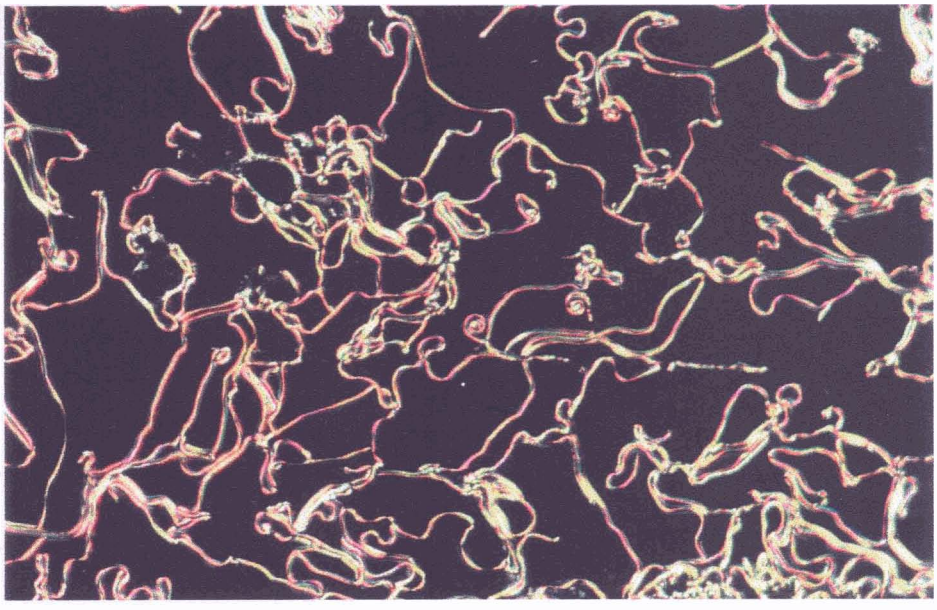

Plate 3.5 : Photomicrograph of compound 7 (series 3.19) showing the spiraling of the corrugated filaments.

Near the transition to the higher temperature phase, the filaments coalesce with each other resulting in a texture as shown in plate 3.6.

Plate 3.6 : Photomicrograph of compound 7 (series 3.19) showing the $UTGB_{C^*}$ texture close to the $UTGB_{C^*} \leftrightarrow N^*$ transition.

On increasing the temperature further, platelet texture characteristic of the N* phase was formed [32].

In cells treated for planar alignment the N* phase exhibited a planar texture. In such samples the twist axis lies perpendicular to the glass plates. As the temperature was lowered, the planar texture of the N* phase changed over to a well-aligned square grid pattern, identical to the one observed for the $UTGB_{C*}$ phase [47]. This pattern is probably a consequence of the two-dimensional undulation of the TGB_{C*}-like blocks. Plate 3.7 shows the square grid pattern of the $UTGB_{C*}$ phase obtained on a cell coated for homogeneous alignment.

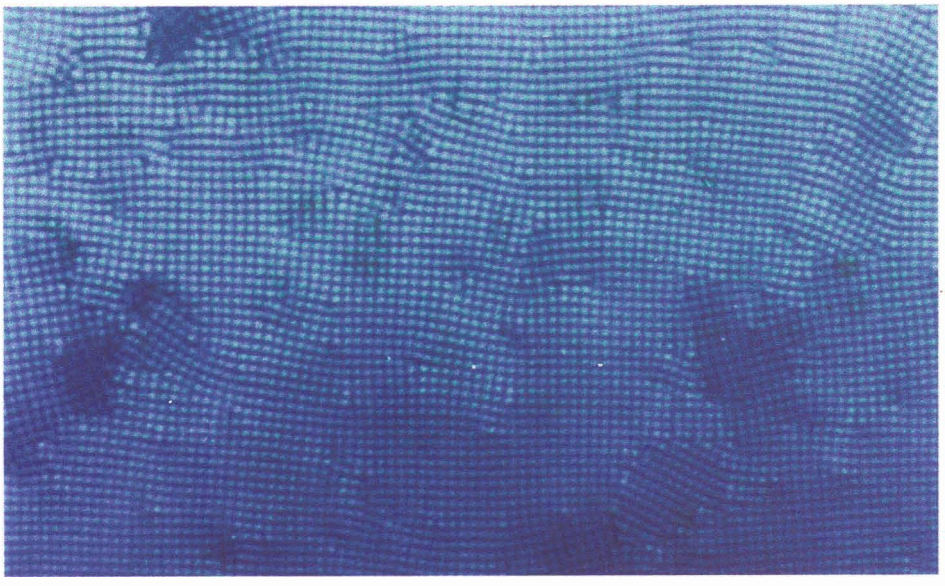

Plate 3.7 : Photomicrograph of compound 8 (series 3.18) showing the square grid pattern of the $UTGB_{C*}$ phase (homogeneously aligned) at 178.0°C.

It is known that in smectic phases molecular chirality can lead to the appearance of different types of long-range director modulated structures [53]. The existence of a phase with the periodic director rotation inside the smectic layer has been theoretically predicted [50,51,52]. Such a phase is believed to be associated with a regular array of defects. Different types of one- and two-dimensional periodic systems of defects were detected in free suspended films of Sm C* materials [53], which can lead to textures having periodic stripes or a square grid pattern. The appearance of square grid pattern in Sm C* phase is an interesting manifestation of molecular chirality.

In order to confirm that the square grid pattern seen in our samples were genuinely due to the new phase and not due to some instability effect in Sm C* phase, the samples were examined in wedge-shaped cells of appropriate thickness (50μ). In such cells, where the thickness varied continuously from one edge of the cell to the other, an array of equidistant Grandjean-Cano (GC) lines formed in the N^* phase as shown in plate 3.8. The texture in between the lines was smooth with gradual colour variation from the thinner to the thicker side of the cell. The colour variation was due to the changes in the helical pitch induced by the treated glass plates.

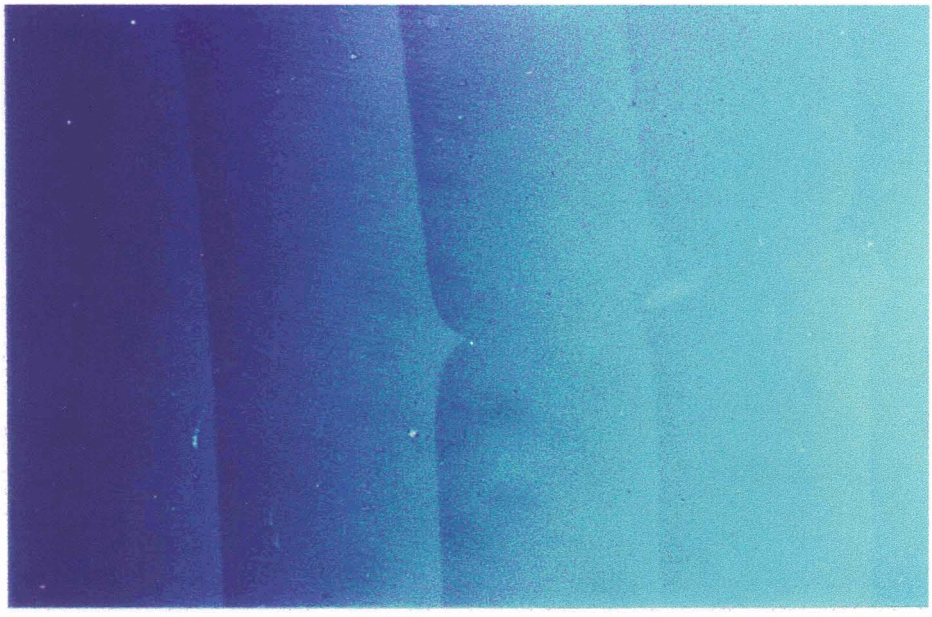

Plate 3.8 : Photomicrograph of the Grandjean-Cano lines formed in the N* phase of compound 3 (series 3.19) on a wedge-shaped cell.

As the temperature was lowered, the square grid pattern began to appear starting from the thinner side of each GC line and filled the entire region as observed previously [47] for the $UTGB_{C^*}$ phase. The array of GC lines continued to exist and the spacing between them continuously increased with the decrease in the temperature. When the transition took place to the Sm C* phase, the GC lines became highly distorted and non-periodic. Plate 3.9 shows the square grid pattern of the $UTGB_{C^*}$ phase in a wedge-shaped cell.

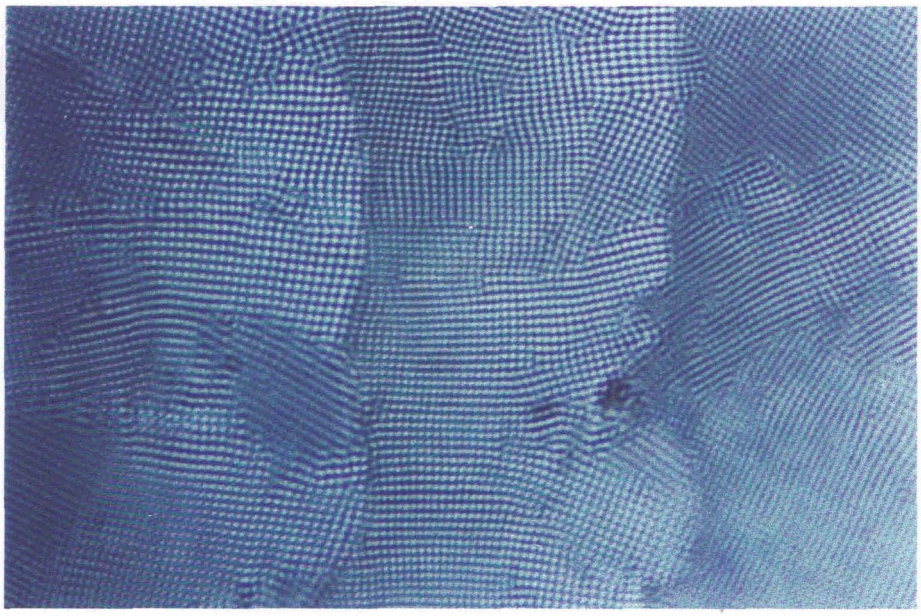

Plate 3.9 : **Photomicrograph of the square grid pattern seen on a wedge-shaped cell.**

The transition temperatures and the corresponding enthalpy values for different transitions obtained from the DSC thermograms for compounds belonging to the series 3.18, 3.19 and 3.20 are summarized in tables 3.3, 3.4 and 3.5 respectively.

All the compounds belonging to the three series **3.18, 3.19** and 3.20 are mesogenic. They have very high clearing temperatures and undergo thermal decomposition at temperatures greater than 230°C. From the tables 3.3 and 3.4 it is seen that the higher homologues (n = 11 to 18) belonging to series 3.18 and 3.19, exhibit the phase sequence Cr u Sm $C^{*} \leftrightarrow UTGB_{C^{*}} \leftrightarrow N^{*}$ on heating. The lowest homologue (n = 8) of series 3.18 shows only a N* phase and homlogues n = 9 and 10 exhibit a monotropic Sm C* phase in addition to the N* phase (table 3.3). The lower homologues of series 3.19 (n = 9 and 10) exhibit only N* and Sm C* phases with the lowest homologue n = 9 showing a monotropic Sm C* and the homologue n = 10 showing an enantiotropic Sm C* phase (table 3.4). In series 3.20 (table 3.5) except for the lowest homologue (n = 7) which shows only a N* phase, the homologues n = 8 to 14 show the phase sequence Cr u Sm $C^{*} \leftrightarrow UTGB_{C^{*}} \leftrightarrow N^{*}$ on heating. Compound 8 (n = 16) exhibits a TGB_{A} phase between the $UTGB_{C^{*}}$ and the N* phase, in addition to the above phase sequence. The $UTGB_{C^{*}}$ phase gets eliminated in the highest homologue (n = 18) of this series, which exhibits the phase sequence Cr u Sm $C^{*} \leftrightarrow Sm\ A \leftrightarrow TGB_{A} \leftrightarrow N^{*}$ on heating.

Table 3.3 : Transition temperatures (°C) and enthalpies (kJ mol^{-1}) for cholesteryl 2-fluoro-4-(4'-n-alkylbenzoyloxy)benzoates.

Compound number	n	Cr	Sm C*	UTGB$_{C*}$	N*	
1	8	. 117.5 *43.3*	-	-		>230 d
2	9	. 119.5 *26.7*	(. 94.0) *0.28*	-		>230 d
3	10	. 117.0 *26.4*	(. 116.0) *0.24*	-		>230 d
4	11	. 116.5 *25.6*	. 124.0 †	. 133.0 *0.19*	.	>230 d
5	12	. 111.0 *24.4*	. 134.5 †	. 146.5 *0.23*	.	>230 d
6	14	. 99.5 ⊗*37.8*	. 158.5 †	. 164 *0.13*	.	>230 d
7	16	. 102.5 *29.0*	- 170.5 †	. 177.5 *0.05*	.	>230 d
8	18	. 100.0 *30.4*	- 177.0 †	. 185.0 *-0.19*	.	>230 d

† : The enthalpy could not be measured; ⊗ : Total enthalpy including any other crystal-crystal transition; ( ) : Indicates a monotropic transition; d : Decomposes.

Table 3.4 : Transition temperatures (°C) and enthalpies (kJ mol^{-1}) for cholesteryl 2-fluoro-4-(4'-n-alkoxybenzoyloxy)benzoates.

Compound number	n	Cr	Sm C*	UTGB$_{C*}$	N*	
1	9	. 112.0 ⊗*45.4*	(. 99.0) *-0.36*	-		>230 d
2	10	. 83.0 *34.1*	. 118.0 *-0.27*	-		>230 d
3	11	. 94.5 *27.2*	. 128.0 †	. 135.5 *0.29*	.	>230 d
4	12	. 111.0 *26.4*	. 133.0 †	. 147.0 *0.21*	.	>230 d
5	14	. 85.5 *27.2*	. 163.0 †	. 172.0 *0.35*	.	>230 d
6	16	. 102.0 *28.1*	. 175.5 †	. 184.0 *0.24*	.	>230 d
7	18	. 86.0 *27.8*	. 181.5 †	. 189.0 †	.	>230 d

† : The enthalpy could not be measured; ⊗ : Total enthalpy including any other crystal-crystal transition; ( ) : Indicates a monotropic transition; d : Decomposes.

Table 3.5 : Transition temperatures (°C) and enthalpies (kJ mol^{-1}) for cholesteryl 2-fluoro-4-(3'-fluoro-4'-n-alkoxybenzoyloxy)benzoates.

Compound number	n	Cr		Sm C*		Sm A		$UTGB_{C*}$		TGB_A		N*	
1	7	.	141.0 ⊗*42.7*	-		-		-		-			>230 d
2	8	.	115.0 ***23.5***	.	121.0 †	-			127 ***0.26***	-			>230 d
3	9	.	115.5 ⊗*28.8*	.	141.0 †	-		.	149.5 ***0.25***	-			>230 d
4	10	.	101.0 ***22.4***	.	155.0 †	-		.	165.0 ***0.34***	-			>230 d
5	11	.	107.0 ⊗*33.8*	.	168.0 †	-		.	178.5 ***0.50***	-			>230 d
6	12	.	110.0 ⊗*70.5*	.	176.5 †	-		.	186.0 ***0.50***	-			>230 d
7	14	.	113.0 ***31.8***	.	191.0 †	-		.	199.0 ***0.10***	-			>230 d
8	16	.	100.5 ***33.7***	.	195.0 t	-		.	196.0 t	.	207.0 t		>230 d
9	18	.	103.0 ***36.4***	.	193.0 †	.	209.5	-			212.5 †		>230 d

† : The enthalpy could not be measured; ⊗ : Total enthalpy including any other crystal-crystal transition; d : Decomposes.

The general mesomorphic trends of the compounds belonging to the three series (3.18, 3.19 and 3.20) have been plotted as a function of temperature *versus* the number of carbon atoms in the terminal n-alkyl/alkoxy chains and depicted in figures 3.11, 3.12 and 3.13 respectively.

The plots show a smooth curve relationship for like transitions. It can be seen from the plots that for all the three series (3.18, 3.19 and 3.20) of compounds, the Sm C* to $UTGB_{C^*}$ transition temperature increases with the increase in the alkyl/alkoxy chain length. This rise is quite sharp for the lower homologues and becomes gradual for the higher homologues. The $UTGB_{C^*}$ to N* transition also shows a similar trend.

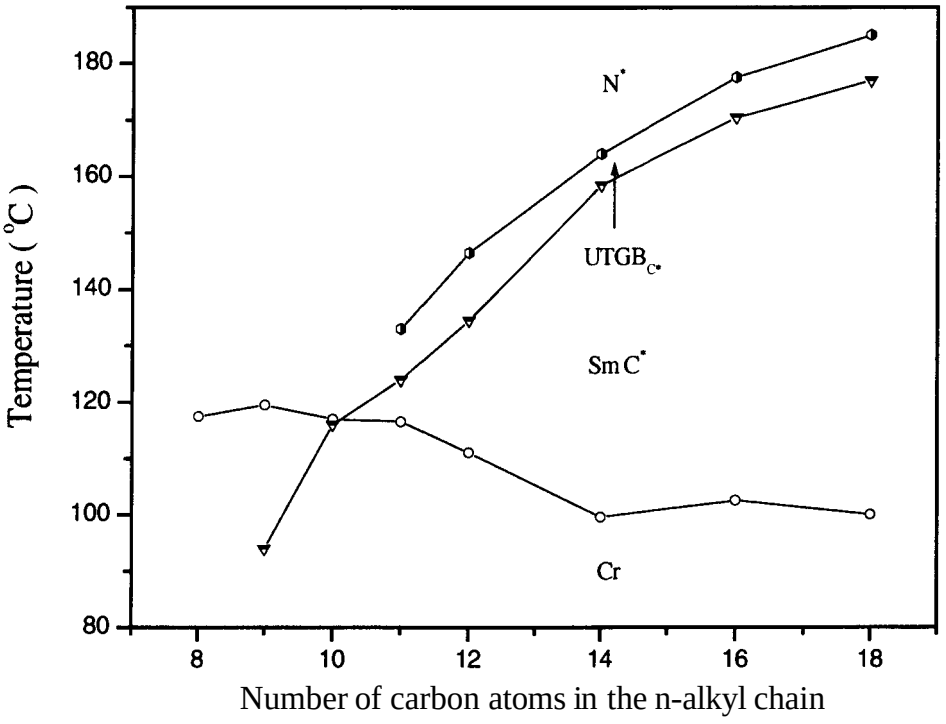

Fig 3.11 : Plot of transition temperatures *versus* the number of carbon atoms in the n-alkyl chain for series 3.18.

In series 3.18 (fig 3.11) and 3.19 (fig 3.12), the $UTGB_{C^*}$ thermal range increases initially on increasing the alkyl chain length from n = 11 to 12 followed by a slight decrease at n = 14 and then remains fairly constant with further increase in the chain length.

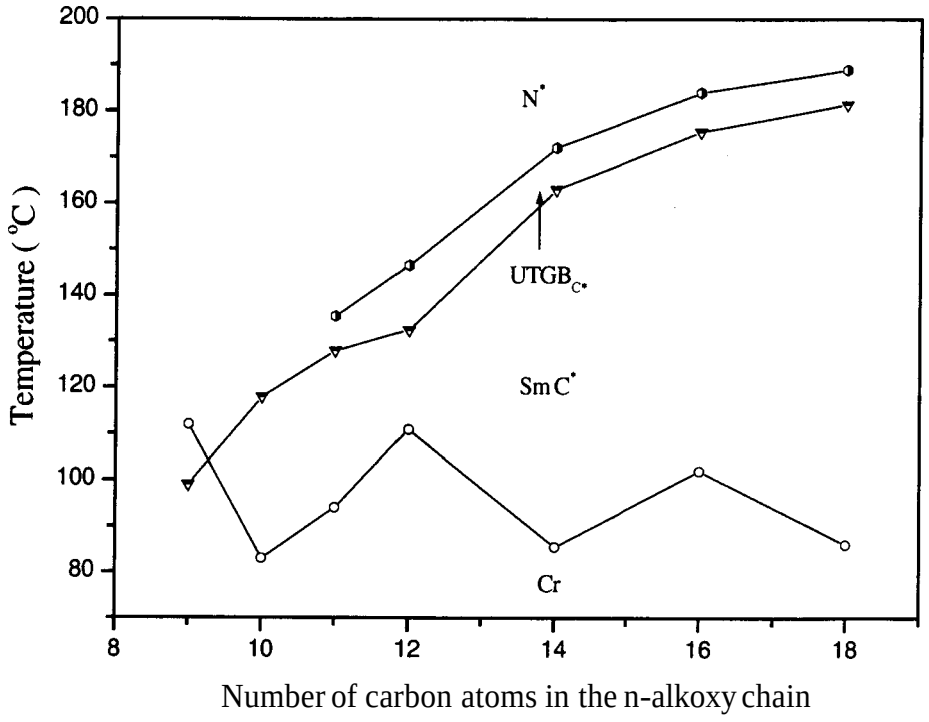

Fig 3.12 : Plot of transition temperatures *versus* number of carbon atoms in the n-alkoxy chain for series 3.19.

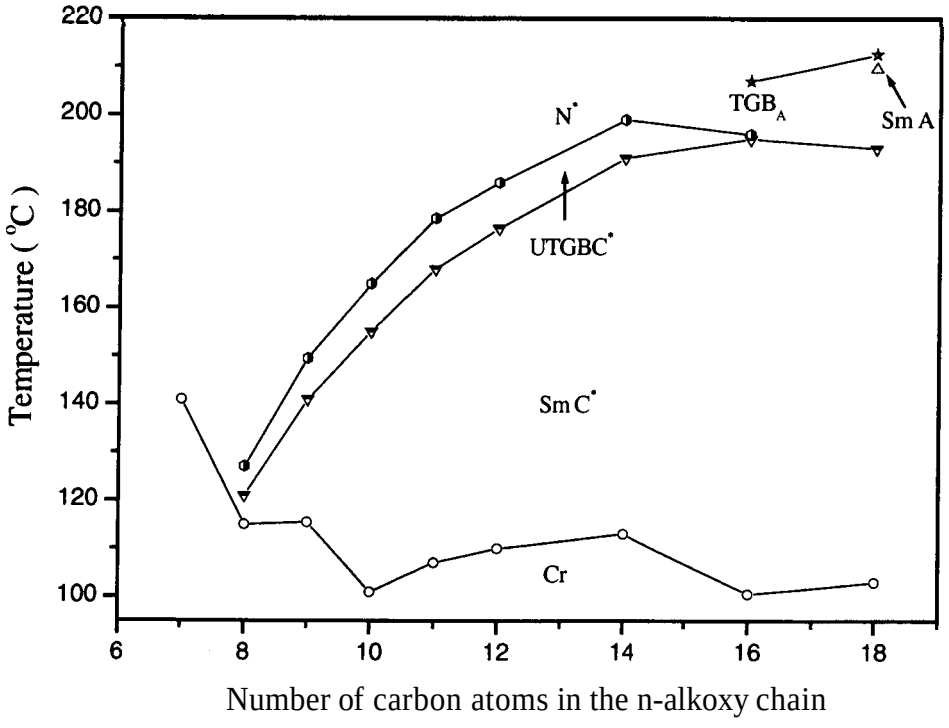

Fig 3.13 : Plot of the number of carbon atoms in the n-alkoxy chain *versus* the transition temperatures for series 3.20.

In series 3.20 (fig 3.13), the thermal range of the $UTGB_{C*}$ phase increases with increase in the chain length up to n = 12, after which there is a decrease. The fall in the range is quite abrupt (from 8°C to 1°C) for compound 8 where TGB_A phase is induced between the $UTGB_{C*}$ and N^* phases. The overall thermal range of the $UTGB_{C*}$ phase in all the three series lies between 1°C and 14°C, with compound 7 of series 3.20 having the least (1°C) and compound 4 of series 3.19 having the largest (14°C) range.

The DSC scan of compound 3 (series 3.19) is shown in figure 3.14. The Sm C* to $UTGB_{C*}$ being a second order transition could not be detected even at rates as low as 0.1°C/min.

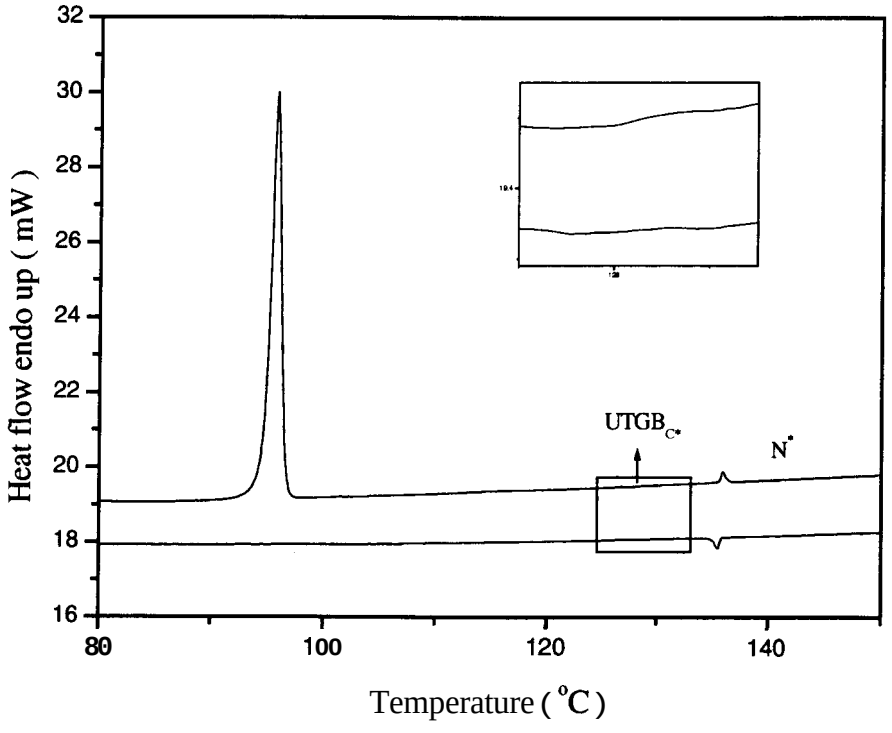

Fig 3.14 : **DSC scan of compound** 3 **(series** 3.19) **at 5°C/min.; inset shows the enlarged view of the box.**

Figure 3.15 shows the IR spectrum of compound 6 (series 3.18). Figures 3.16 and 3.17 depict the ^1H NMR spectra of compounds 7 (series 3.19) and 3.28 which have cholesteryl and cholestanol groups respectively as the chiral moieties. It can be seen that in figure 3.17, the multiplet at $\delta = 5.4$ppm, due to the olefinic hydrogen present in **the** cholesteryl moiety has disappeared indicating the absence of the double bond in compound 3.28.

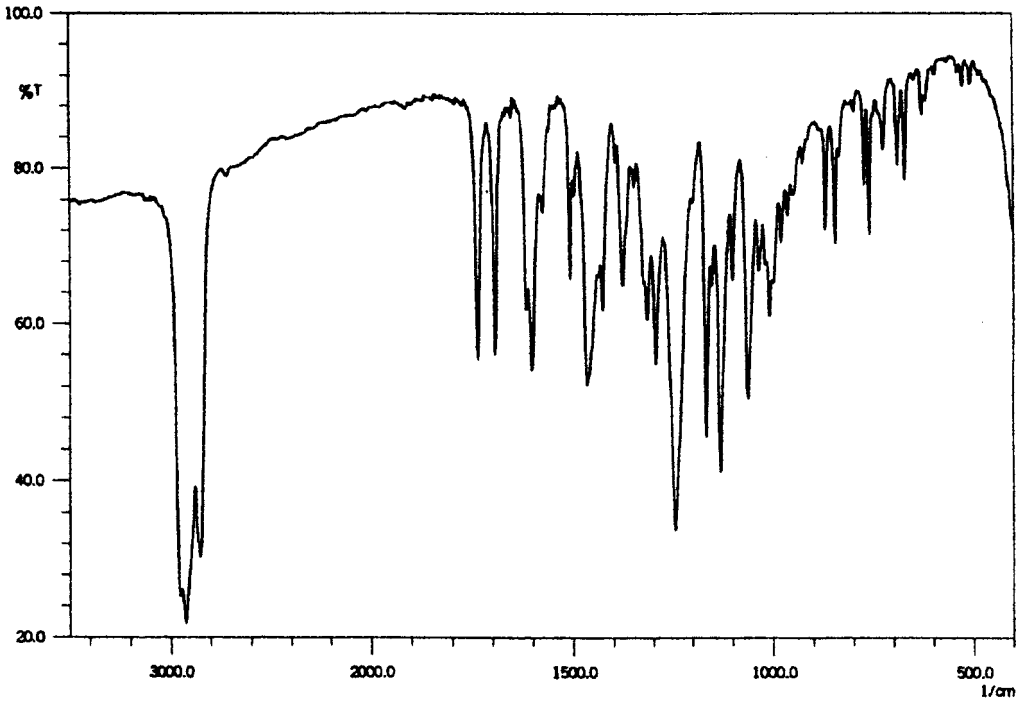

Fig 3.15 : Infrared spectrum of compound 6 (series 3.18).

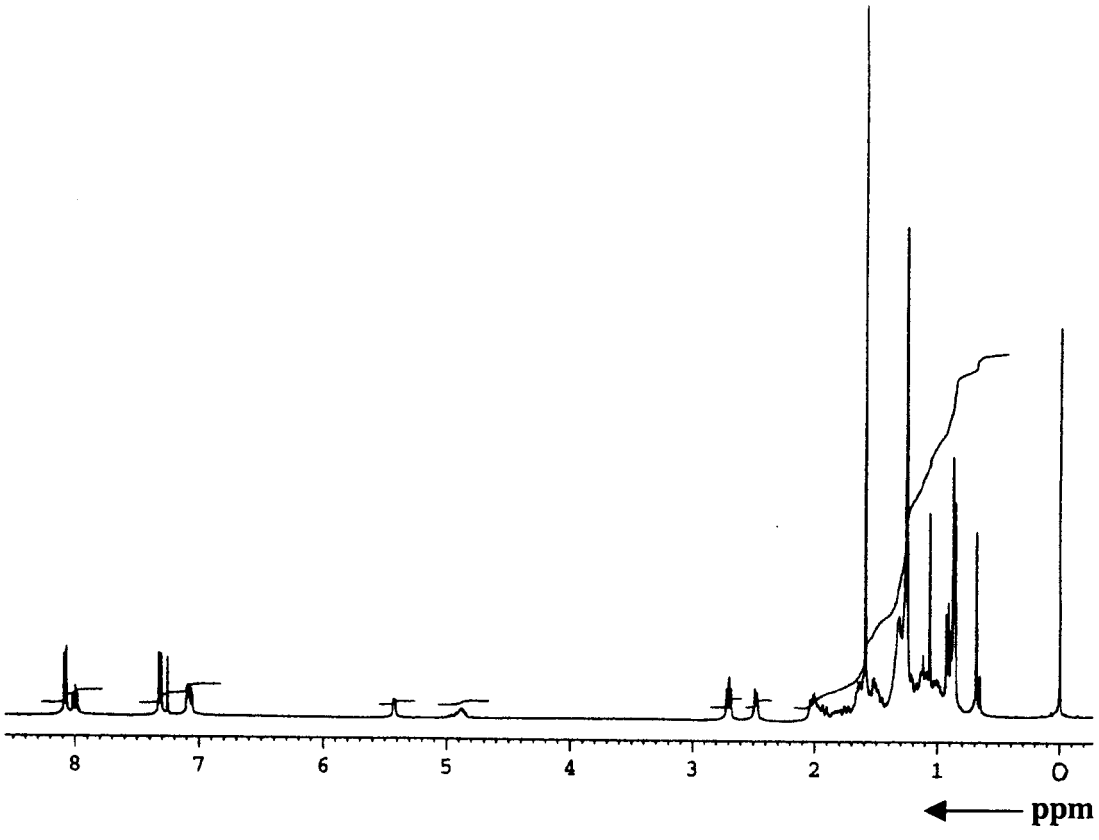

Fig 3.16 : ^{1}H NMR spectrum of compound 7 (series 3.19).

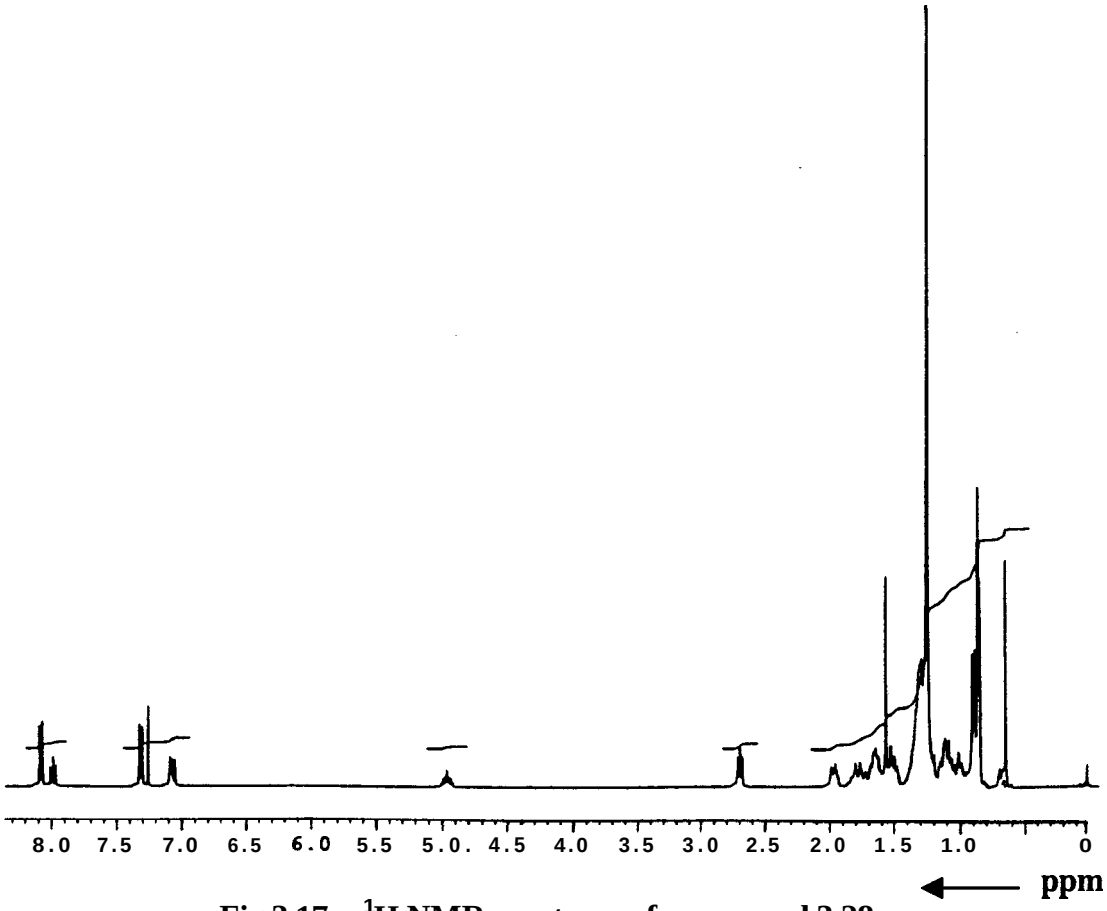

Fig 3.17 : ^{1}H NMR spectrum of compound 3.28.

Since these are the first examples of single component systems exhibiting this new phase, the exact molecular structural requirements for a compound to exhibit this new phase are still not very clear. In order to examine this aspect we carried out the synthesis of a few other related compounds which are used for comparative studies in the subsequent sections.

3.5.1 Effect of lateral substitution on the occurrence and stability of the UTGB$_{C*}$ phase:

As seen earlier, the type and the position of the lateral substituent on the core can bring about dramatic changes in the type and stability of the mesophase that a potential material may exhibit. Also it is a known fact that in most cases fluorine is chosen to be the most suitable lateral substituent due to its unique properties which have already been discussed.

Consider the following compounds,

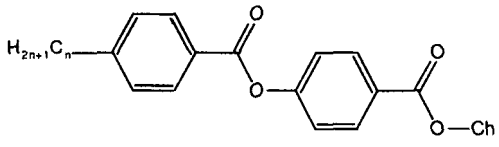

n = 16 : Cr 112.0 SmC^* 175.0 Sm A 200.0 TGB_A 200.0 N* >220 decompose. (3.21)

n = 18 : Cr 99.0 SmC^* 165.0 Sm A 200.5 TGB_A 205.0 N*>220 decompose. (3.22)

The mesomorphic behaviour of the above two compounds (3.21 and 3.22) can be compared with those of the corresponding homologues (compounds 7 and 8) of series 3.18. Compounds 3.21 and 3.22, which do not have any lateral substituents (parent compounds) on the core, exhibit the phase sequence Cr ↔ SmC^* ↔ Sm A ↔ TGB_A ↔ N*. In addition to this, compound **3.21** shows a very short-range blue phase whose temperature could not be determined due to thermal decomposition of the compound. However, in compounds 7 and 8 (series 3.18, table 3.3) which have a lateral fluoro substituent *ortho* to the carboxylate group close to the chiral moiety, the TGB_A and Sm A phases get eliminated and instead the new $UTGB_{C*}$ phase is induced between the Sm C* and N* phases. Apart from this a considerable increase in the Sm C* phase stability is also observed. As has been discussed earlier the probable reason for the above observation could be due to the following two effects:

(a) Increase in the transverse moment adjacent to the chiral center, which favours the formation and stabilization of the tilted phases.

(b) Increase in the molecular chirality brought about by the restricted rotation of the chiral moiety with respect to the long molecular axis, due to the presence of the lateral group adjacent to the chiral moiety, which favours the formation of the TGB phases.

A similar comparison can be made between the compounds of series 3.19 (table 3.4) and 3.20 (table 3.5). In series 3.19, the compounds have a fluoro substituent close to the chiral group. Except for the lower homologues (compounds 1 and 2), all the other homologues exhibit the phase sequence Cr↔SmC^*↔$UTGB_{C*}$↔N^*. The compounds in series 3.20 have two fluoro substituents, one *ortho* to the carboxylate group close to the chiral moiety and the other *ortho* to the terminal n-alkoxy chain.

Except for the lowest homologue (compoundl) the phase sequence observed is similar for compounds 2 to 7. It is interesting to note that in this series, compound 8 shows a TGB_A phase in between the $UTGB_{C*}$ and N* phases accompanied by a dramatic fall in the temperature range of the $UTGB_{C*}$ phase (1°C). However, in compound 9 (highest homologue), the $UTGB_{C*}$ phase gets eliminated and it shows the following phase sequence Cr ↔ SmC^* ↔ Sm A ↔ TGB_A ↔ N*. In other words, for longer chain lengths (n = 16 and 18), the presence of fluoro substituent *ortho* to the terminal alkoxy chain destabilizes the $UTGB_{C*}$ phase.

Comparing the transition temperatures of compound 8 of series 3.19 (table 3.4) and compound 3.23 we can draw a similar conclusion.

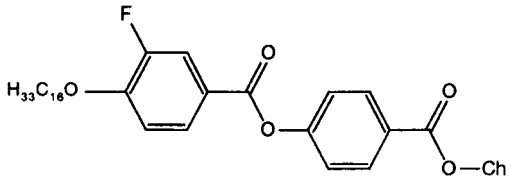

Cr 117.0 SmC^* 181.5 Sm **A** 240.4 TGB_A 240.5 N*>245 decompose

(3.23)

It can be seen from table 3.4 that compound 8 which has a lateral fluoro substituent close to the chiral moiety shows the phase sequence $Cr \leftrightarrow SmC^* \leftrightarrow UTGB_{C*} \leftrightarrow N^*$. The thermal range of $UTGB_{C*}$ phase is about 8.5°C. However, when the position of the fluoro substituent in compound 8 is changed such that it is *ortho* to the terminal alkoxy chain (compound **3.23)**, this phase gets eliminated; instead TGB_A and Sm **A** phases are induced between the Sm C* and N* phases. Also this compound shows a short-range blue phase but the temperature of this phase could not be determined due to thermal decomposition of the compound.

The effect of the position of the lateral fluoro substituent in compounds having two fluoro substituents can be illustrated by comparing the mesomorphic properties of compound 8 of series 3.20 (table 3.5) and compound 3.24.

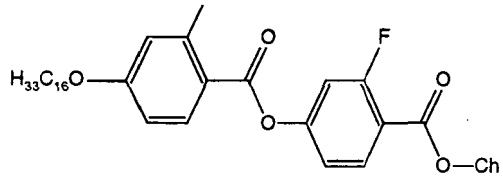

Cr 90.0 SmC^* 153.0 $UTGB_{C*}$ 160.5 N*>220 decompose

(3.24)

From table 3.5, it is seen that compound 8 which has two fluoro substituents, one close to the chiral moiety and the other *ortho* to the alkoxy chain exhibits a TGB_A phase between the Sm C*and $UTGB_{C*}$ phases. Also the thermal range of the $UTGB_{C*}$ phase is about 1°C. However, in compound 3.24, in which one of the fluoro substituents is facing the inner core of the molecule, the TGB_A phase gets eliminated while the $UTGB_{C*}$ phase is stabilized (7.5°C) as compared to compound 8.

The effect of the type of lateral substituents on the occurrence of the new phase can be examined by considering the following examples:

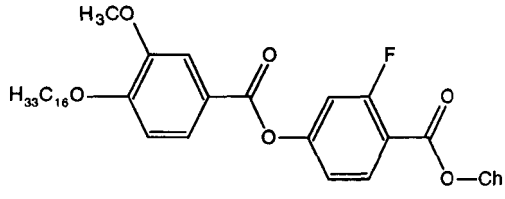

Cr 139.0 N^* 221.6 BP 221.8 I

(3.25)

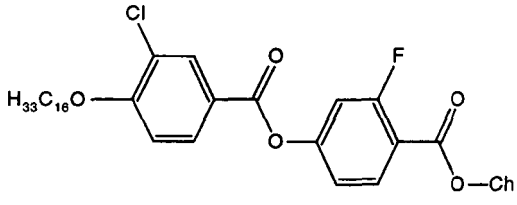

Cr 113.0 SmC^* 170.5 $UTGB_{C*}$ 183.0 N*>240 decompose

(3.26)

The mesomorphic properties of compound 8 of series 3.20 (table 3.5) can be compared with those of compounds 3.25 and 3.26. Compound 8 exhibits the following phase sequence $Cr \leftrightarrow SmC^* \leftrightarrow UTGB_{C*} \leftrightarrow TGB_A \leftrightarrow N^*$. The $UTGB_{C*}$ phase

in this compound exists over a very short-range (1°C). It is interesting to note that when the lateral fluoro substituent close to the terminal alkoxy chain of compound 8 is replaced by a chloro group (compound **3.26**), the TGB_A phase gets eliminated and there is a significant enhancement in the stability of the $UTGB_{C*}$ (12.5°C) phase. However, when it is replaced by a methoxy group (compound 3-25), the Sm C* and TGB phases are eliminated and this compound shows only N* and blue phases. This may be due to a significant fall in the length to breadth ratio of the molecule owing to a large van der Waals radius of the methoxy group, which is responsible for the destabilization (suppression) of all the smectic phases.

Therefore, it can be concluded that presence of a chloro substituent *ortho* to the terminal alkoxy chain along with a fluoro substituent close to the chiral moiety in two ring systems with cholesteryl group as the chiral moeity favours the formation and stabilizes the $UTGB_{C*}$ phase when compared to a difluoro substituted system.

3.5.2 Effect of the type of chiral moiety on the occurrence of the $UTGB_{C*}$ phase:

As we have seen in our discussion earlier, the type of chiral moiety present in the molecule is also one of the prime factors that govern the formation of the TGB phases. This effect with reference to the $UTGB_{C*}$ phase can be illustrated in the following examples:

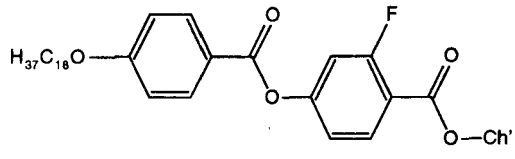

Cr 91.5 SmC^* 177.5 $UTGB_{C*}$ 180.5 N*>230 decompose

(3.27)

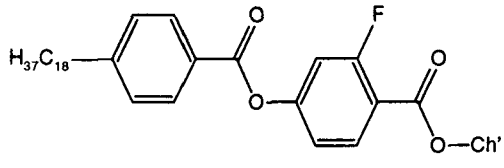

Cr 81.0 SmC^* 165.5 Sm **A** 172.5 TGB_A 179.5 N^* >225 decompose

(3.28)

Ch' = Cholestanol moiety.

The structure of the cholestanol moiety used as the chiral group in **3.27** and **3.28** is shown in figure 3.18

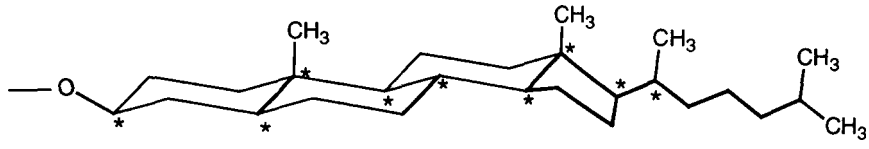

Fig 3.18 : Cholestanol moiety.

Compound **3.27** can be compared with compound 7 of series **3.19** (table 3.4). The two differ from each other in the type of chiral moiety they have. Both the compounds exhibit the phase sequence $Cr \leftrightarrow SmC^{*} \leftrightarrow UTGB_{C^{*}} \leftrightarrow N^{*}$. However, in compound **3.27,** which has cholestanol moiety as the chiral group, a decrease in both the transition temperatures and the $UTGB_{C^{*}}$ thermal range (3°C) is observed.

A similar comparative study can be carried out between compound **3.28** and its analogue, compound 8 of series **3.18** (table3.4). It is quite interesting to note that unlike compound 8 (table 3.4), compound **3.28** which has cholestanol moiety as the chiral group does not exhibit the $UTGB_{C^{*}}$ phase and instead shows a phase sequence $Cr \leftrightarrow SmC^{*} \leftrightarrow Sm\ A \leftrightarrow TGB_{A} \leftrightarrow N^{*}$. The thermal range of TGB_{A} phase is about 7°C. Also it can be seen that in this compound a decrease in the transition temperatures is observed.

Therefore the overall decrease in the polarity of the molecule due to the reduction of the double bond present in the cholesteryl moiety may be the reason for the above observations.

In order to explore the possibility of getting the $UTGB_{C^{*}}$ phase without using cholesteryl group as the chiral moiety, we carried out the synthesis of the following compounds:

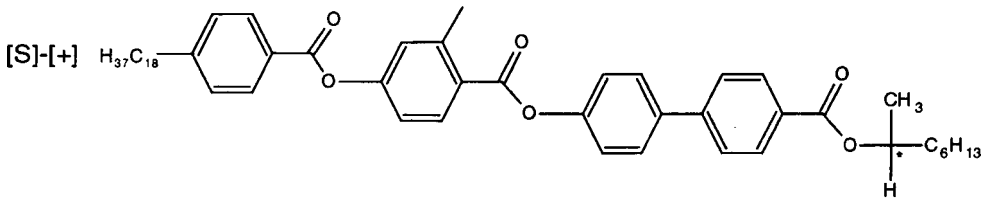

Cr 69.0 Sm C* 156.5 Sm A 165.9 TGB_A 166.0 I

(3.29)

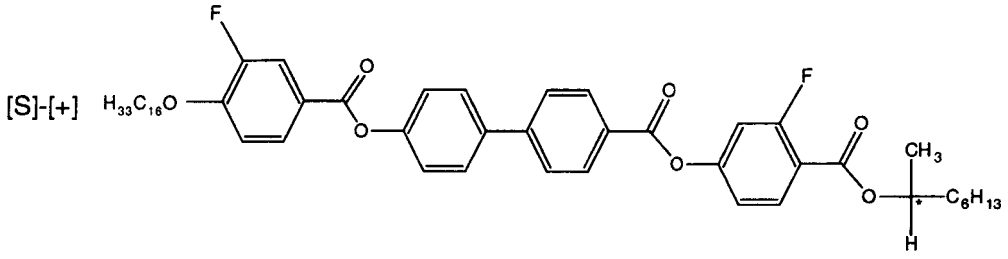

Cr 79.0 Sm C* 201.0 Sm A 215.0 I

(3.30)

As can be seen, compound 3.29 shows a very short-range (0.1°C) TGB_A phase and compound 3.30 did not exhibit any of the TGB phases but showed only Sm A and Sm C* phases.

From the above results, the following observations have been made:

(1) In two ring systems with cholesterol as the chiral moiety, presence of a lateral fluoro substituent *ortho* to the carboxylate group close to the chiral moiety is a prerequisite for the compounds to exhibit $UTGB_{C^*}$ phase. On the other hand, a lateral fluoro substituent *ortho* to the terminal alkoxy chain does not favour the formation of the $UTGB_{C^*}$ phase (compound 3.23).

(2) Sufficiently long **alkyl/alkoxy** chain lengths (n = 211) are required for the mono fluoro substituted systems to exhibit this new phase.

(3) In difluoro substituted systems, the $UTGB_{C^*}$ phase gets destabilized in higher homologues (n = 16,18) (table 3.5). However, replacement of the fluoro substituent *ortho* to the terminal alkoxy chain by:

(a) **A** chloro substituent favours the formation of the new phase (compound 3.26).

(b) **A** methoxy group destabilizes all the smectic phases (compound 3.25).

(4) **A** difluoro system having one fluoro substituent towards the inner core of the molecule and the other close to the chiral center (compound 3.24) is found to stabilize the $UTGB_{C*}$ phase as compared to one in which one of the fluoro substituent is *ortho* to the terminal alkoxy chain and the other *ortho* to the carboxylate group close to the chiral center.

(5) Replacement of the cholesteryl group with the cholestanol group as the chiral moiety decreases the stability of the $UTGB_{C*}$ phase (compounds 3.27 and 3.28).

Since single component systems with groups other than cholesterol/cholestanol as chiral moieties and exhibiting this phase are not known, careful study is required to unearth the molecular structural requirements for a compound to exhibit this novel $UTGB_{C*}$ phase.

3.6 **X-ray diffraction studies:**

X-ray diffraction studies were carried out on powder samples. The sample under investigation was filled in the cholesteric phase into a 0.7mm diameter Lindemann capillary tube and the ends of the capillary were flame sealed. The sample was then mounted in a computer controlled oven and the collimated x-ray beam from a Rigaku 18kW rotating anode x-ray generator was impinged on the sample. The scattered intensity was recorded on an image plate. The sample to detector distance was 226.16mm.

The diffraction patterns were recorded on cooling the sample (compound 4, series 3.18) from the cholesteric phase down to the Sm C* phase. The exposure time given was about sixty minutes. In the N* phase, a uniform ring with a rather broad radial intensity distribution was obtained. The real space periodicity, which produced this ring, was roughly equal to the total molecular length. On lowering the temperature into the $UTGB_{C*}$ phase, the ring became quite sharp when compared to that obtained from the N* phase for the same exposure time. In this phase an intense uniform sharp

ring was observed in the small angle region, which indicates a well-organized layer structure and a broad diffuse halo was observed in the wide angle region, which is characteristic of a fluid-like packing of the molecules. The periodicity of the structure was calculated to be 34.8Å, which is less than the total molecular length. This clearly indicates that in this phase the molecules are tilted with respect to the layer normal as in the case of a Sm C^* phase. The tilt angle was calculated to be 34°, assuming the molecule to be in a conformation as shown in figure 3.19 with the n-alkoxy chain fully extended.

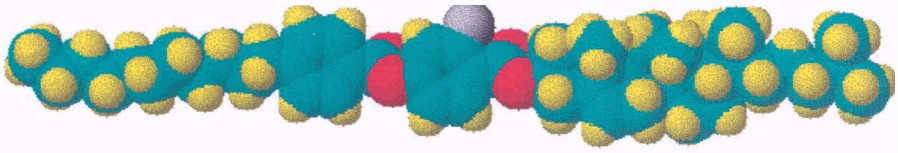

Fig 3.19

On further cooling to the Sm C* phase, a pattern similar to that seen for $UTGB_{C*}$ phase was observed. Therefore, in a powder diffraction technique, the Sm C* and $UTGB_{C*}$ phases could not be distinguished. However, it is quite evident from the x-ray studies that the phase below the N* phase is a tilted lamellar phase. This result along with the fact that GC lines are seen on a square grid background in a wedge-shaped cell similar to what was observed by Pramod et *al.* [47], confirms the presence of the new $UTGB_{C*}$ phase in our compounds.

A plot of the intensity *versus* θ for the $UTGB_{C*}$ phase of compound 4 (series 3.18) is shown in figure 3.19. The plot shows a well pronounced Bragg peak in the small angle region and a broad diffuse peak in the wide angle region.

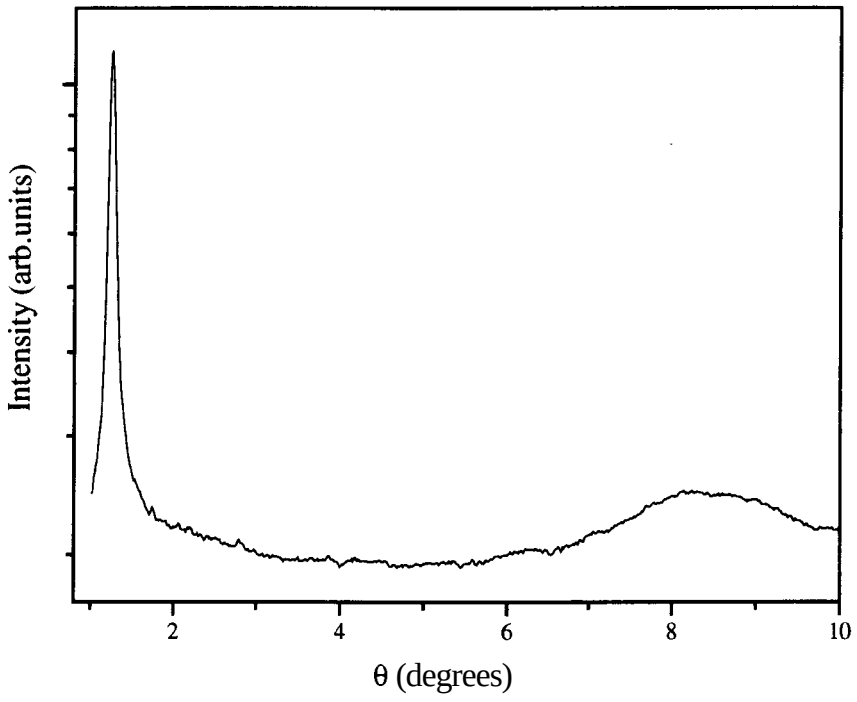

Fig 3.20 : **Plot of intensity** *versus* θ **for the UTGB$_{C*}$ phase of compound 4 (series** 3.18).

3.7 **Helical pitch measurement (p):**

The pitch measurement for the UTGB$_{C*}$ phase was carried out following a procedure described in part I(sec 3.3.1) of this chapter. Thus, the sample was taken in a wedge-shaped cell of appropriate thickness (50μ) and the spacing between the GC lines was measured as a function of temperature by cooling the sample at a slow rate (0.2°C/min). The pitch value was calculated using the formula given in section 3.3.1. Figures 3.21, 3.22 and 3.23 show the plots of variation of pitch with temperature for compounds 4(series **3.18**), 3(series 3.19) and 4(series 3.20) respectively.

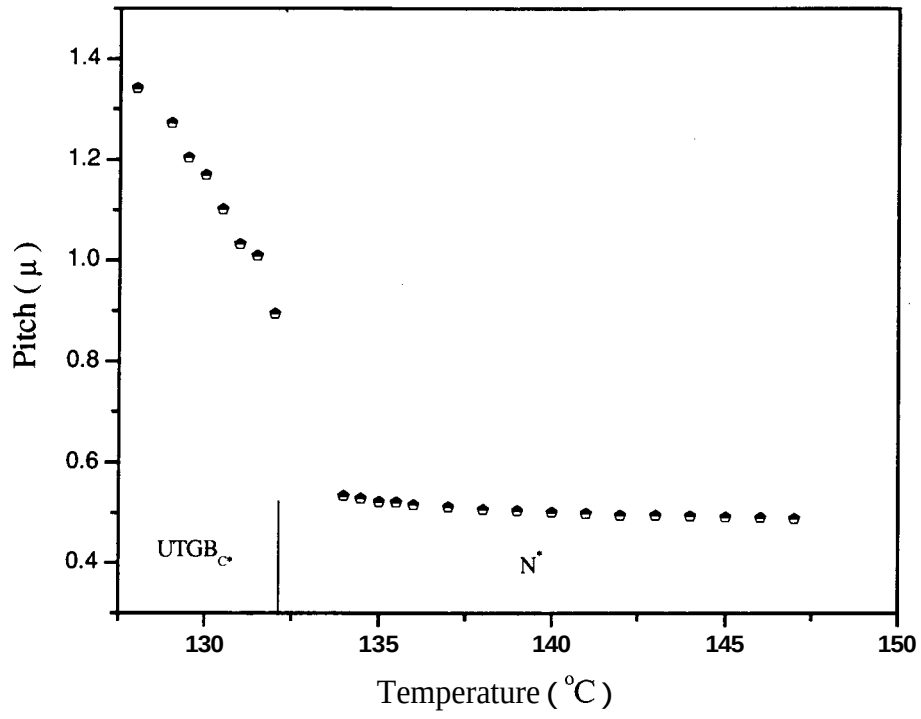

Fig 3.21 : Plot of pitch *versus* temperature of compound 4 (series 3.18). The vertical line indicates the transition temperature.

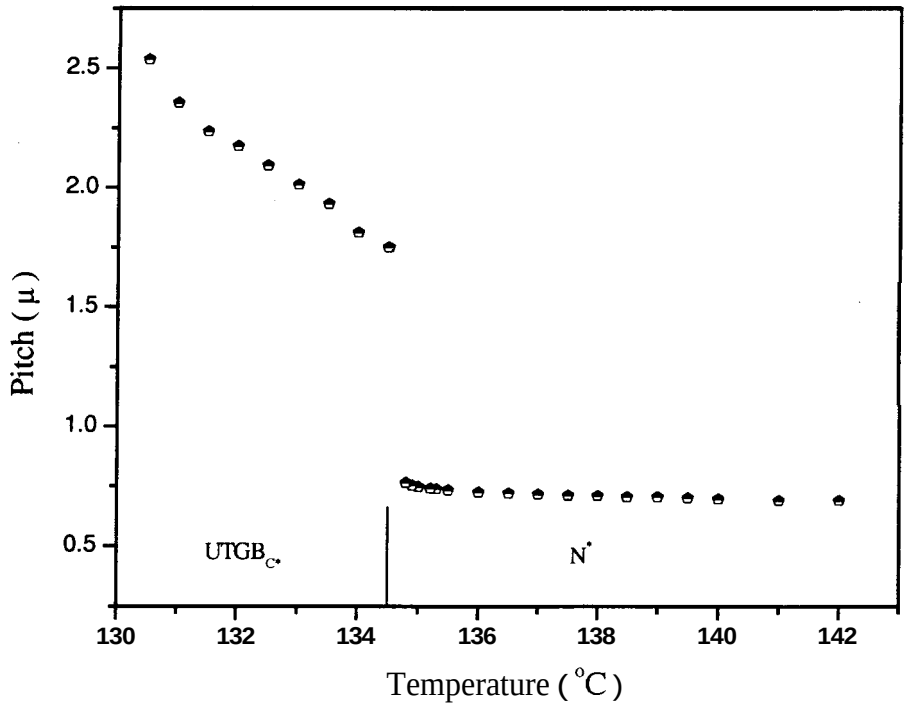

Fig 3.22 : Plot of pitch *versus* temperature of compound 3 (series 3.19).

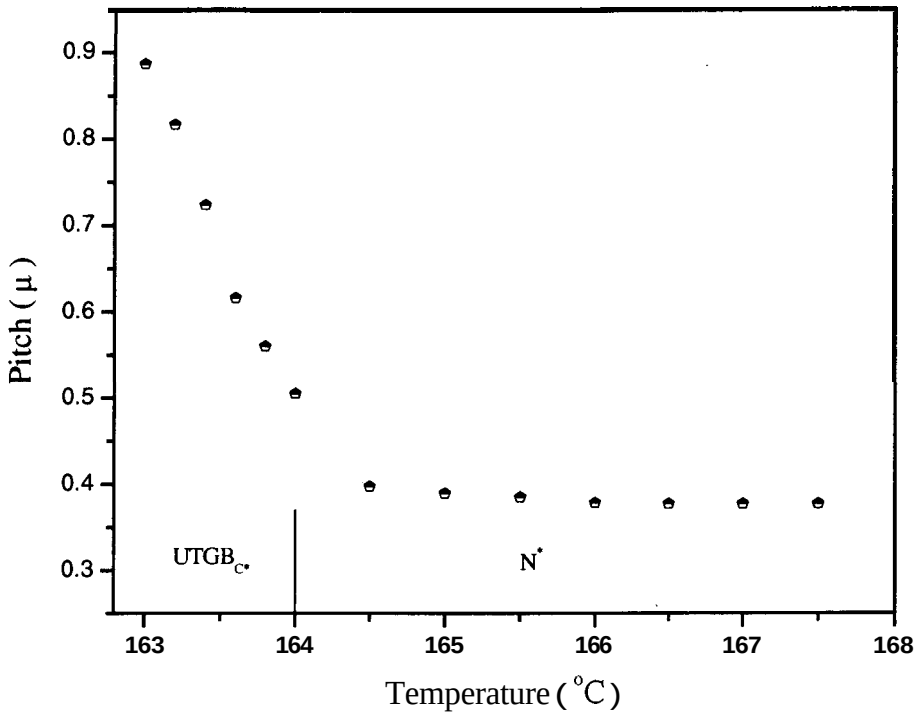

Fig 3.23 : Plot of pitch *versus* temperature of compound 4 (series 3.20).

From the plots it is clear that within the N* phase there is hardly any variation in the pitch value. At the N* ↔ **UTGB$_{C*}$** phase transition, a very significant jump in the pitch value can be seen. The magnitude of this jump varied depending on the nature of the compound. Therefore, a discontinuity in the slope was seen at the transition point. On cooling further into the **UTGB$_{C*}$** phase, the pitch increased quite sharply. The variation of pitch with temperature followed a trend similar to that observed by Pramod et al. [47] for the mixture of compounds.

3.8 Experimental

The 2-fluoro-4-n-alkoxybenzoic acids were prepared following a procedure described by Gray, Hogg and Lacey [31]. The procedures for the preparation of the 2-fluoro-4-benzyloxybenzoic acid and 3-fluoro-4-n-alkoxybenzoic acids are given in section 2.3 of chapter 2. The 4-n-alkyl/alkoxybenzoic acids were prepared following a procedure described earlier [48,49].

Cholesteryl 2-fluoro-4-benzyloxybenzoate, (3.31)

This was prepared following an esterification procedure of Hassner and Alexanian [54]. Thus, a mixture of 2-fluoro-4-benzyloxybenzoic acid (2g, 8.1mmol), cholesterol (3.46g, 8.9mmol), DMAP (0.01g, 0.8mmol) and dry dichloromethane (20ml) was stirred for five minutes. To this mixture, was added DCC (1.84g, 8.9mmol) and stirring continued overnight at room temperature. The N,N'-dicyclohexylurea formed was filtered off and the filtrate diluted with dichloromethane (50ml). The resultant solution was washed with 5% aqueous acetic acid (2X20ml), water (3X30ml) and dried over Na_2SO_4. The solvent was removed from the filtered solution to yield a residue which was purified by column chromatography on silica gel using chloroform:petroleum ether (60:40) as eluent to yield pure cholesteryl 2-fluoro-4-benzyloxybenzoate as a white solid which was crystallized from n-butanol (3.4g, 68.76%), m.p. 154.7°C; $[\alpha]_D^{25} = 0.9°$ (16mg/ml in $CHCl_3$); ν_{max} (nujol): 2900, 1700, 1620, 1460, 1370, 1280, and 1130 cm^{-1}; **δ:** 1.08-2.0 (26H, m, $10XCH_2$, 6XCH), 0.68 (3H, s, tertiary CH_3), 1.05 (3H, s, tertiary CH_3), 0.85, 0.87 (3H, d) and 0.857, 0.873 (3H, d) [$RCH(\underline{CH_3})_2$], 0.91-0.93 (3H, d, $R_1R_2CH(\underline{CH_3})$), 2.44-2.45 (2H, m, allylic H), 5.41 (1H, m, olefinic H), 5.1 (2H, s, $ArCH_2OAr$), 4.82-4.84 (1H, m, -CHOCOAr), 6.68-7.9 (8H, m, ArH).

Cholesteryl 2-fluoro-4-hydroxybenzoate, (3.32)

A mixture of cholesteryl 2-fluoro-4-benzyloxybenzoate (2.9g, 4.75mmol) dissolved in 1,4-dioxane (50ml) and 5% Pd-C catalyst (1.0g) was stirred in an atmosphere of hydrogen at 50°C till the calculated quantity of hydrogen was absorbed.

The reaction mixture was then filtered and removal of solvent under reduced pressure yielded a white solid which was crystallized from 1,4-dioxane:petroleum ether mixture (2.24g, 90%); m.p. 255.4-256.7°C (decomposes); $[\alpha]_D^{25}$ = -0.25°(40mg/ml in THF); ν_{max} (nujol): 3350, 2950, 1690, 1620, 1460, 1380, 1270, and 1140 cm^{-1}; *6:* 1.08-2.0 (26H, m, $10XCH_2$, 6XCH), 0.68 (3H, s, tertiary CH_3), 1.05 (3H, s, tertiary CH_3), 0.85, 0.87 (3H, d) and 0.857, 0.873 (3H, d) [$RCH(\underline{CH_3})_2$], 0.91-0.93 (3H, d, $R_1R_2CH(\underline{CH_3})$), 2.44-2.45 (2H, m, allylic H), 5.41 (1H, m, olefinic H), 5.1 (2H, s, $ArCH_2OAr$), 4.0-4.9 (1H, m, -CHOCOAr), 6.6-7.9 (4H, m, ArH), 3.7 (1H, s, ArOH).

Cholesteryl 4-benzyloxybenzoate, (3.33)

This was prepared following a procedure described for compound 3.31. Yield, 80%; m.p. 160°C; $[\alpha]_D^{25}$ = 2.32°(8mg/ml in $CHCl_3$); ν_{max} (nujol): 2900, 1700, 1600, 1450, 1380, 1270, and 1160 cm^{-1}; 6: 1.O-2.03 (26H, m, $10XCH_2$, 6XCH), 0.68 (3H, s, tertiary CH_3), 1.06 (3H, s, tertiary CH_3), 0.854, 0.87 (3H, d) and 0.858, 0.875 (3H, d) [$RCH(\underline{CH_3})_2$], 0.91-0.93 (3H, d, $R_1R_2CH(\underline{CH_3})$), 2.43-2.45 (2H, m, allylic H), 5.41 (1H, m, olefinic H), 5.1 (2H, s, $ArCH_2OAr$), 4.81-4.83 (1H, m, -CHOCOAr), 6.97-8.0 (9H, m, ArH).

Cholesteryl 4-hydroxybenzoate, (3.34)

This was prepared following a procedure described for compound 3.32. Yield, 75%; m.p. 240-242°C (decomposes); $[\alpha]_D^{25}$ = 2.8°(12.8mg/ml in THF); ν_{max} (nujol): 3330, 2900, 1670, 1600, 1450, 1370, 1260, and 1160 cm^{-1}; 6: 1.3-2.4 (26H, m, $10XCH_2$, 6XCH), 0.87 (3H, s, tertiary CH_3), 1.25 (3H, s, tertiary CH_3), 1.05, 1.07 (3H, d) and 1.058, 1.075 (3H, d) [$RCH(\underline{CH_3})_2$], 1.11-1.13 (3H, d, $R_1R_2CH(\underline{CH_3})$), 2.63-2.65 (2H, m, allylic H), 5.55-5.6 (1H, m, olefinic H), 4.89-5.0 (1H, m, -CHOCOAr), 7.07-8.09 (5H, m, ArH), 3.1 (1H, s, ArOH).

Cholestanyl 2-fluoro-4-benzyloxybenzoate, (3.35)

This was prepared following a procedure described for compound 3.31. Yield, 82%; m.p. 148.8'~; $[\alpha]_D^{25}$ = 10.8°(11.5mg/ml in $CHCl_3$); ν (nujol): 2900, 1700, 1620, 1460, 1380, 1280, and 1140 cm^{-1}; 6: 0.88-1.9 (34H, m, $12XCH_2$, 7XCH, $1XCH_3$), 0.58 (3H, s, tertiary CH_3), 0.784, 0.8 (3H, d) and 0.798, 0.8 (3H, d) [$RCH(\underline{CH_3})_2$], 0.82-0.84 (3H, d, $R_1R_2CH(\underline{CH_3})$), 5.02 (2H, s, $ArCH_2OAr$), 4.82-4.87 (1H, m, -CHOCOAr), 6.97-8.0 (8H, m, ArH).

Cholestanyl 2-fluoro-4-hydroxybenzoate, (3.36)

This was prepared following a procedure described for compound 3.32. Yield, 75%; m.p. 218.5°C; $[\alpha]_D^{25}$ = 11.9°(17.8mg/ml in acetone); ν_{max} (nujol): 3300, 2900, 1690, 1620, 1460, 1380, 1280, and 1140 cm^{-1}; 6: 0.88-1.9 (34H, m, $12XCH_2$, 7XCH, $1XCH_3$), 0.83 (3H, s, tertiary CH_3), 0.997, 1.014 (3H, d) and 1.01, 1.03 (3H, d) [$RCH(\underline{CH_3})_2$], 1.06-1.08 (3H, d, $R_1R_2CH(\underline{CH_3})$), 4.91-5.06 (1H, m, -CHOCOAr), 6.74-7.98 (4H, m, ArH), 3.07 (1H, s, ArOH).

Cholesteryl 2-fluoro-4-n-octadecyloxybenzoate

A mixture of 2-fluoro-4-n-octadecyloxybenzoic acid (0.2g, 0.5mmol), cholesterol (0.21g, 0.54mmol), DCC (0.11g, 0.54mmol), DMAP (0.06g, 0.05mmol) and dry dichloromethane was stirred overnight at room temperature. The precipitated N,N'-dicyclohexylurea was filtered off and the filtrate diluted with dichloromethane (10ml). The combined organic solution was washed with 5% aqueous acetic acid (2X5ml), water (2X10ml) and dried over Na_2SO_4. The solvent was removed from the filtered solution to yield a residue which was purified by column chromatography on silica gel using chloroform:petroleum ether as eluent to yield pure cholesteryl 2-fluoro-4-n-octadecyloxybenzoate as a white solid which was crystallized repeatedly from 2-methoxyethanol (0.3g, 80%); m.p. 94.0°C; $[\alpha]_D^{25}$ = 0.8° (9.9mg/ml in $CHCl_3$); ν_{max} (nujol): 2900, 1700, 1610, 1450, 1370, 1250, and 1130 cm^{-1}; 6: 1.08-2.16 (58H, m, $26XCH_2$, 6XCH), 0.68 (3H, s, tertiary CH_3), 1.055 (3H, s, tertiary CH_3), 0.853, 0.87 (3H, d) and 0.858, 0.875 (3H, d) [$RCH(\underline{CH_3})_2$], 0.89-0.92 (6H, m, $2XCH_3$), 2.44-2.46 (2H, m, allylic H), 5.41 (1H, m, olefinic H), 3.95-3.98 (2H, t, $ArOCH_2$-), 4.8-4.9 (1H, m, -CHOCOAr), 6.57-7.87 (3H, m, ArH).

The physical data of the cognate preparations of the other cholesteryl 2-fluoro-4-n-alkoxybenzoates are given below.

Cholesteryl 2-fluoro-4-n-hexadecyloxybenzoate

Yield, 75%; m.p. 85.0°C; $[\alpha]_D^{25}$ = -0.5' (14mg/ml in $CHCl_3$); ν (nujol): 2900, 1700, 1610, 1450, 1370, 1250, and 1130 cm''; 6: 1.08-2.16 (54H, m, $24XCH_2$, 6XCH), 0.68 (3H, s, tertiary CH_3), 1.055 (3H, s, tertiary CH_3), 0.853, 0.87 (3H, d) and 0.858, 0.875 (3H, d) [$RCH(\underline{CH_3})_2$], 0.89-0.92 (6H, m, $2XCH_3$), 2.44-2.46 (2H, m, allylic H), 5.41 (1H, m, olefinic H), 3.95-3.98 (2H, t, $ArOCH_2$-), 4.8-4.9 (1H, m, -CHOCOAr), 6.57-7.87 (3H, m, ArH).

Cholesteryl 2-fluoro-4-n-tetradecyloxybenzoate

Yield, 78%; m.p. 105.0°C; $[\alpha]_D^{25}$ = -0.3° (15.7mg/ml in $CHCl_3$); ν (nujol): 2900, 1700, 1610, 1450, 1370, 1250, and 1130 cm^{-1}; 6: 1.08-2.16 (50H, m, $22XCH_2$, 6XCH), 0.68 (3H, s, tertiary CH_3), 1.055 (3H, s, tertiary CH_3), 0.853, 0.87 (3H, d) and 0.858, 0.875 (3H, d) [$RCH(\underline{CH_3})_2$], 0.89-0.92 (6H, m, $2XCH_3$), 2.44-2.46 (2H, m, allylic H), 5.41 (1H, m, olefinic H), 3.95-3.98 (2H, t, $ArOCH_2$-), 4.8-4.9 (1H, m, -CHOCOAr), 6.57-7.87 (3H, m, ArH).

Cholesteryl 2-fluoro-4-n-dodecyloxybenzoate

Yield, 74%; m.p. 118.5°C; $[\alpha]_D^{25}$ = -0.5" (16mg/ml in $CHCl_3$); ν_{max} (nujol): 2900, 1700, 1610, 1450, 1370, 1250, and 1130 cm^{-1}; 6: 1.08-2.16 (46H, m, $20XCH_2$, 6XCH), 0.68 (3H, s, tertiary CH_3), 1.055 (3H, s, tertiary CH_3), 0.853, 0.87 (3H, d) and 0.858, 0.875 (3H, d) [$RCH(\underline{CH_3})_2$], 0.89-0.92 (6H, m, $2XCH_3$), 2.44-2.46 (2H, m, allylic H), 5.41 (1H, m, olefinic H), 3.95-3.98 (2H, t, $ArOCH_2$-), 4.8-4.9 (1H, m, -CHOCOAr), 6.57-7.87 (3H, m, ArH).

Cholesteryl 2-fluoro-4-(4'-n-octadecylbenzoyloxy)benzoate

The esterification of compound 3.32 and 4-n-octadecylbenzoic acid was carried out following a procedure described for compound 3.31. Yield, 87.2%; m.p. 100.0°C;

$[\alpha]_D^{25}$ = 1.9° (10mg/ml in $CHCl_3$); ν_{max} (nujol): 2950, 1735, 1700, 1460, 1290, 1250 and 1050 cm^{-1}; 6: 1.08-2.16 (58H, m, 26XCH_2, 6XCH), 0.68 (3H, s, tertiary CH_3), 1.06 (3H, s, tertiary CH_3), 0.855, 0.87 (3H, d) and 0.859, 0.876 (3H, d) [RCH($\underline{CH_3}$)$_2$], 0.89-0.93 (6H, m, 2XCH_3), 2.46-2.48 (2H, m, allylic H), 5.42 (1H, m, olefinic H), 2.6-2.7 (2H, t, ArCH_2-), 4.86-5.0 (1H, m, -CHOCOAr), 7.0-8.0 (7H, m, ArH).

The physical data of the cognate preparations of the other cholesteryl 2-fluoro-4-(4'-n-alkylbenzoyloxy)benzoates are given below.

Cholesteryl 2-fluoro-4-(4'-n-hexadecylbenzoyloxy)benzoate

Yield, 81.5%; m.p. 102.5°C; $[\alpha]_D^{25}$ = 2.2' (9mg/ml in $CHCl_3$); ν_{max} (nujol): 2950, 1735, 1700, 1460, 1290, 1250 and 1050 cm^{-1}; 6: 1.08-2.16 (54H, m, 24XCH_2, 6XCH), 0.68 (3H, s, tertiary CH_3), 1.06 (3H, s, tertiary CH_3), 0.855, 0.87 (3H, d) and 0.859, 0.876 (3H, d) [RCH($\underline{CH_3}$)$_2$], 0.89-0.93 (6H, m, 2XCH_3), 2.46-2.48 (2H, m, allylic H), 5.42 (1H, m, olefinic H), 2.6-2.7 (2H, t, ArCH_2-), 4.86-5.0 (1H, m, -CHOCOAr), 7.0-8.0 (7H, m, ArH).

Cholesteryl 2-fluoro-4-(4'-n-tetradecylbenzoyloxy)benzoate

Yield, 85%; m.p. 99.5°C; $[\alpha]_D^{25}$ = 3.0° (10mg/ml); ν_{max} (nujol): 2950, 1735, 1700, 1460, 1290, 1250 and 1050 cm^{-1}; 6: 1.08-2.16 (50H, m, 22XCH_2, 6XCH), 0.68 (3H, s, tertiary CH_3), 1.06 (3H, s, tertiary CH_3), 0.855, 0.87 (3H, d) and 0.859, 0.876 (3H, d) [RCH($\underline{CH_3}$)$_2$], 0.89-0.93 (6H, m, 2XCH_3), 2.46-2.48 (2H, m, allylic H), 5.42 (1H, m, olefinic H), 2.6-2.7 (2H, t, ArCH_2-), 4.86-5.0 (1H, m, -CHOCOAr), 7.0-8.0 (7H, m, ArH).

Cholesteryl 2-fluoro-4-(4'-n-dodecylbenzoyloxy)benzoate

Yield, 89.3%; m.p. 111°C; $[\alpha]_D^{25}$ = 0.92° (10.8mg/ml in $CHCl_3$); ν (nujol): 2950, 1735, 1700, 1460, 1290, 1250 and 1050 cm^{-1}; 6: 1.08-2.16 (46H, m, 20XCH_2, 6XCH), 0.68 (3H, s, tertiary CH_3), 1.06 (3H, s, tertiary CH_3), 0.855,

0.87 (3H, d) and 0.859, 0.876 (3H, d) [RCH($\underline{CH_3}$)$_2$], 0.89-0.93 (6H, m, 2XCH_3), 2.46-2.48 (2H, m, allylic H), 5.42 (1H, m, olefinic H), 2.6-2.7 (2H, t, ArCH_2-), 4.86-5.0 (1H, m, -CHOCOAr), 7.0-8.0 (7H, m, ArH).

Cholesteryl 2-fluoro-4-(4'-n-undecylbenzoyloxy)benzoate

Yield, 89.5%; m.p. 116.5°C; $[\alpha]_D^{25}$ = 0.96° (11.4mg/ml in $CHCl_3$); ν (nujol): 2950, 1735, 1700, 1460, 1290, 1250 and 1050 cm^{-1}; δ: 1.08-2.16 (44H, m, 19XCH_2, 6XCH), 0.68 (3H, s, tertiary CH_3), 1.06 (3H, s, tertiary CH_3), 0.855, 0.87 (3H, d) and 0.859, 0.876 (3H, d) [RCH($\underline{CH_3}$)$_2$], 0.89-0.93 (6H, m, 2XCH_3), 2.46-2.48 (2H, m, allylic H), 5.42 (1H, m, olefinic H), 2.6-2.7 (2H, t, ArCH_2-), 4.86-5.0 (1H, m, -CHOCOAr), 7.0-8.0 (7H, m, ArH).

Cholesteryl 2-fluoro-4-(4'-n-decylbenzoyloxy)benzoate

Yield, 86%; m.p. 117.0°C; $[\alpha]_D^{25}$ = 2.08° (12mg/ml in $CHCl_3$); ν_{max} (nujol): 2950, 1735, 1700, 1460, 1290, 1250 and 1050 cm^{-1}; δ: 1.08-2.16 (42H, m, 18XCH_2, 6XCH), 0.68 (3H, s, tertiary CH_3), 1.06 (3H, s, tertiary CH_3), 0.855, 0.87 (3H, d) and 0.859, 0.876 (3H, d) [RCH($\underline{CH_3}$)$_2$], 0.89-0.93 (6H, m, 2XCH_3), 2.46-2.48 (2H, m, allylic H), 5.42 (1H, m, olefinic H), 2.6-2.7 (2H, t, ArCH_2-), 4.86-5.0 (1H, m, -CHOCOAr), 7.0-8.0 (7H, m, ArH).

Cholesteryl 2-fluoro-4-(4'-n-nonylbenzoyloxy)benzoate

Yield,90%; m.p. 119.5°C; $[\alpha]_D^{25}$ = 2.6' (15.5mg/ml in $CHCl_3$); ν (nujol): 2950, 1735, 1700, 1460, 1290, 1250 and 1050 cm^{-1}; δ: 1.08-2.16 (40H, m, 17XCH_2, 6XCH), 0.68 (3H, s, tertiary CH_3), 1.06 (3H, s, tertiary CH_3), 0.855, 0.87 (3H, d) and 0.859, 0.876 (3H, d) [RCH($\underline{CH_3}$)$_2$], 0.89-0.93 (6H, m, 2XCH_3), 2.46-2.48 (2H, m, allylic H), 5.42 (1H, m, olefinic H), 2.6-2.7 (2H, t, ArCH_2-), 4.86-5.0 (1H, m, -CHOCOAr), 7.0-8.0 (7H, m, ArH).

Cholesteryl 2-fluoro-4-(4'-n-octylbenzoyloxy)benzoate

Yield, 90%; m.p. 117.5°C; $[\alpha]_D^{25}$ = 2.76° (16.6mg/ml in $CHCl_3$); ν_{max} (nujol): 2950, 1735, 1700, 1460, 1290, 1250 and 1050 cm^{-1}; δ: 1.08-2.16 (38H, m, 16XCH_2, 6XCH), 0.68 (3H, s, tertiary CH_3), 1.06 (3H, s, tertiary CH_3), 0.855, 0.87 (3H, d) and 0.859, 0.876 (3H, d) [RCH($\underline{CH_3}$)$_2$], 0.89-0.93 (6H, m, 2XCH_3), 2.46-2.48 (2H, m, allylic H), 5.42 (1H, m, olefinic H), 2.6-2.7 (2H, t, ArCH_2-), 4.86-5.0 (1H, m, -CHOCOAr), 7.0-8.0 (7H, m, ArH).

Cholesteryl 2-fluoro-4-(4'-n-octadecyloxybenzoyloxy)benzoate

This was prepared by esterifying compound 3.32 with 4-n-octadecyloxybenzoic acid using a procedure described for compound 3.31. Yield, 85%; m.p. 86°C; $[\alpha]_D^{25}$ = 3.24' (10.8mg/ml in $CHCl_3$); ν_{max} (nujol): 2950, 1740, 1710, 1600, 1460, 1280, 1240, 1130, 1160 and 1060 cm^{-1}; δ: 1.08-2.17 (58H, m, 26XCH_2, 6XCH), 0.68 (3H, s, tertiary CH_3), 1.06 (3H, s, tertiary CH_3), 0.855, 0.864 (3H, d) and 0.859, 0.87 (3H, d) [RCH($\underline{CH_3}$)$_2$], 0.88-0.92 (6H, m, 2XCH_3), 2.46-2.48 (2H, m, allylic H), 5.43 (1H, m, olefinic H), 4.0-4.05 (2H, t, ArOCH_2-), 4.8-5.0 (1H, m, -CHOCOAr), 7.05-8.1 (7H, m, ArH).

The physical data of the cognate preparations of the other cholesteryl 2-fluoro-4(4'-alkoxybenzoyloxy)benzoates are given below.

Cholesteryl 2-fluoro-4-(4'-n-hexadecyloxybenzoyloxy)benzoate

Yield, 85%; m.p. 102.0°C; $[\alpha]_D^{25}$ = 2.36' (11mg/ml in $CHCl_3$); ν_{max} (nujol): 2950, 1740, 1710, 1600, 1460, 1280, 1240, 1130, 1160 and 1060 cm^{-1}; δ: 1.08-2.17 (54H, m, 24XCH_2, 6XCH), 0.68 (3H, s, tertiary CH_3), 1.06 (3H, s, tertiary CH_3), 0.855, 0.864 (3H, d) and 0.859, 0.87 (3H, d) [RCH($\underline{CH_3}$)$_2$], 0.88-0.92 (6H, m, 2XCH_3), 2.46-2.48 (2H, m, allylic H), 5.43 (1H, m, olefinic H), 4.0-4.05 (2H, t, ArOCH_2-), 4.8-5.0 (1H, m, -CHOCOAr), 7.05-8.1 (7H, m, ArH).

Cholesteryl 2-fluoro-4-(4'-n-tetradecyloxybenzoyloxy)benzoate

Yield, 86%; m.p. 85.5°C; $[\alpha]_D^{25}$ = 2.89' (11.4mg/ml in $CHCl_3$); ν_{max} (nujol): 2950, 1740, 1710, 1600, 1460, 1280, 1240, 1130, 1160 and 1060 cm^{-1}; **6:** 1.08-2.17 (50H, m, 22XCH_2, 6XCH), 0.68 (3H, s, tertiary CH_3), 1.06 (3H, s, tertiary CH_3), 0.855, 0.864 (3H, d) and 0.859, 0.87 (3H, d) [RCH($\underline{CH_3}$)$_2$], 0.88-0.92 (6H, m, 2XCH_3), 2.46-2.48 (2H, m, allylic H), 5.43 (1H, m, olefinic H), 4.0-4.05 (2H, t, ArOCH_2-), 4.8-5.0 (1H, m, -CHOCOAr), 7.05-8.1 (7H, m, ArH).

Cholesteryl 2-fluoro-4-(4'-n-dodecyloxybenzoyloxy)benzoate

Yield, 82%; m.p. 111.0°C; $[\alpha]_D^{25}$ = 2.92' (11.6mg/ml in $CHCl_3$); ,v (nujol): 2950, 1740, 1710, 1600, 1460, 1280, 1240, 1130, 1160 and 1060 cm^{-1}; **6:** 1.08-2.17 (46H, m, 20XCH_2, 6XCH), 0.68 (3H, s, tertiary CH_3), 1.06 (3H, s, tertiary CH_3), 0.855, 0.864 (3H, d) and 0.859, 0.87 (3H, d) [RCH($\underline{CH_3}$)$_2$], 0.88-0.92 (6H, m, 2XCH_3), 2.46-2.48 (2H, m, allylic H), 5.43 (1H, m, olefinic H), 4.0-4.05 (2H, t, ArOCH_2-), 4.8-5.0 (1H, m, -CHOCOAr), 7.05-8.1 (7H, m, ArH).

Cholesteryl 2-fluoro-4-(4'-n-undecyloxybenzoyloxy)benzoate

Yield, 80%; m.p. 94.5°C; $[\alpha]_D^{25}$ = 2.73' (11.7mg/ml in $CHCl_3$); ,v (nujol): 2950, 1740, 1710, 1600, 1460, 1280, 1240, 1130, 1160 and 1060 cm^{-1}; **6:** 1.08-2.17 (44H, m, 19XCH_2, 6XCH), 0.68 (3H, s, tertiary CH_3), 1.06 (3H, s, tertiary CH_3), 0.855, 0.864 (3H, d) and 0.859, 0.87 (3H, d) [RCH($\underline{CH_3}$)$_2$], 0.88-0.92 (6H, m, 2XCH_3), 2.46-2.48 (2H, m, allylic H), 5.43 (1H, m, olefinic H), 4.0-4.05 (2H, t, ArOCH_2-), 4.8-5.0 (1H, m, -CHOCOAr), 7.05-8.1 (7H, m, ArH).

Cholesteryl 2-fluoro-4-(4'-n-decyloxybenzoyloxy)benzoate

Yield, 83%; m.p. 83.0°C; $[\alpha]_D^{25}$ = 2.86° (13.9mg/ml in $CHCl_3$); ν_{max} (nujol): 2950, 1740, 1710, 1600, 1460, 1280, 1240, 1130, 1160 and 1060 cm^{-1}; **6:** 1.08-2.17 (42H, m, 18XCH_2, 6XCH), 0.68 (3H, s, tertiary CH_3), 1.06 (3H, s, tertiary CH_3), 0.855, 0.864 (3H, d) and 0.859, 0.87 (3H, d) [RCH($\underline{CH_3}$)$_2$], 0.88-0.92 (6H, m, 2XCH_3), 2.46-2.48 (2H, m, allylic H), 5.43 (1H, m, olefinic H), 4.0-4.05 (2H, t, ArOCH_2-), 4.8-5.0 (1H, m, -CHOCOAr), 7.05-8.1 (7H, m, ArH).

Cholesteryl 2-fluoro-4-(4'-n-nonyloxybenzoyloxy)benzoate

Yield, 85%; m.p. 112.0°C; $[\alpha]_D^{25}$ = 1.74° (14.9mg/ml in $CHCl_3$); ν_{max} (nujol): 2950, 1740, 1710, 1600, 1460, 1280, 1240, 1130, 1160 and 1060 cm^{-1}; 6: 1.08-2.17 (40H, m, 17XCH_2, 6XCH), 0.68 (3H, s, tertiary CH_3), 1.06 (3H, s, tertiary CH_3), 0.855, 0.864 (3H, d) and 0.859, 0.87 (3H, d) [RCH($\underline{CH_3}$)$_2$], 0.88-0.92 (6H, m, 2XCH_3), 2.46-2.48 (2H, m, allylic H), 5.43 (1H, m, olefinic H), 4.0-4.05 (2H, t, ArOCH_2-), 4.8-5.0 (1H, m, -CHOCOAr), 7.05-8.1 (7H, m, ArH).

Cholesteryl 4-(3'-fluoro-4'-n-hexadecyloxybenzoyloxy)benzoate

Yield,' 84%; m.p. 117.0°C; $[\alpha]_D^{25}$ = 0.82' (11mg/ml in $CHCl_3$); ν_{max} (nujol): 2950, 1740, 1710, 1600, 1460, 1280, 1240, 1130, 1160 and 1060 cm^{-1}; 6: 1.1-2.06 (54H, m, 24XCH_2, 6XCH), 0.688 (3H, s, tertiary CH_3), 1.07 (3H, s, tertiary CH_3), 0.855, 0.872 (3H, d) and 0.859, 0.876 (3H, d) [RCH($\underline{CH_3}$)$_2$], 0.89-0.92 (6H, m, 2XCH_3), 2.45-2.47 (2H, m, allylic H), 5.43 (1H, m, olefinic H), 4.1-4.13 (2H, t, ArOCH_2-), 4.87 (1H, m, -CHOCOAr), 7.0-8.1 (7H, m, ArH).

Cholesteryl 2-fluoro-4-(3'-fluoro-4'-n-tetradecyloxybenzoyloxy)benzoate

This was prepared by esterifying compound 3.32 with 3-fluoro-4-n-tetradecyloxybenzoicacid following a procedure described for compound 3.31. Yield, 91.8%; m.p. 113.0°C; $[\alpha]_D^{25}$ = 1.9° (10.5mg/ml in $CHCl_3$); ν_{max} (nujol): 2950, 1740, 1700, 1620, 1470, 1120, 1180, 1290,1250 and 1060 cm^{-1}; 6: 1.09-2.17 (50H, m, 22XCH_2, 6XCH), 0.687 (3H, s, tertiary CH_3), 1.064 (3H, s, tertiary CH_3), 0.855, 0.872 (3H, d) and 0.86, 0.877 (3H, d) [RCH($\underline{CH_3}$)$_2$], 0.895-0.929 (6H, m, 2XCH_3), 2.465-2.485 (2H, m, allylic H), 5.42-5.43 (1H, m, olefinic H), 4.1-4.13 (2H, t, ArOCH_2-), 4.85-4.89 (1H, m, -CHOCOAr), 7.0-8.27 (6H, m, ArH).

The physical data of the cognate preparations of the other cholesteryl 2-fluoro-4-(3'-fluoro-4'-n-alkoxybenzoyloxy)benzoates are given below.

Cholesteryl 2-fluoro-4-(3'-fluoro-4'-n-octadecyloxybenzoyloxy)benzoate

Yield, 92%; m.p. 103°C; $[\alpha]_D^{25}$ = 2.91' (9.6mg/ml in $CHCl_3$); ν_{max} (nujol): 2950, 1740, 1700, 1620, 1470, 1120, 1180, 1290,1250 and 1060 cm^{-1}; 6: 1.09-2.17 (58H, m, $26XCH_2$, 6XCH), 0.687 (3H, s, tertiary CH_3), 1.064 (3H, s, tertiary CH_3), 0.855, 0.872 (3H, d) and 0.86, 0.877 (3H, d) [$RCH(\underline{CH_3})_2$], 0.895-0.929 (6H, m, $2XCH_3$), 2.465-2.485 (2H, m, allylic H), 5.42-5.43 (1H, m, olefinic H), 4.1-4.13 (2H, t, $ArOCH_2$-), 4.85-4.89 (1H, m, -CHOCOAr), 7.0-8.27 (6H, m, ArH).

Cholesteryl 2-fluoro-4-(3'-fluoro-4'-n-hexadecyloxybenzoyloxy)benzoate

Yield, 85%; m.p. 100.5°C; $[\alpha]_D^{25}$ = 3.61° (9.4mg/ml in $CHCl_3$); ν_{max} (nujol): 2950, 1740, 1700, 1620, 1470, 1120, 1180, 1290,1250 and 1060 cm^{-1}; 6: 1.09-2.17 (54H, m, $24XCH_2$, 6XCH), 0.687 (3H, s, tertiary CH_3), 1.064 (3H, s, tertiary CH_3), 0.855, 0.872 (3H, d) and 0.86, 0.877 (3H, d) [$RCH(\underline{CH_3})_2$], 0.895-0.929 (6H, m, $2XCH_3$), 2.465-2.485 (2H, m, allylic H), 5.42-5.43 (1H, m, olefinic H), 4.1-4.13 (2H, t, $ArOCH_2$-), 4.85-4.89 (1H, m, -CHOCOAr), 7.0-8.27 (6H, m, ArH).

Cholesteryl 2-fluoro-4-(3'-fluoro-4'-n-dodecyloxybenzoyloxy)benzoate

Yield, 90%; m.p. 110.0°C; $[\alpha]_D^{25}$ = 0.7° (9.9mg/ml in $CHCl_3$); ν_{max} (nujol): 2950, 1740, 1700, 1620, 1470, 1120, 1180, 1290,1250 and 1060 cm^{-1}; 6: 1.09-2.17 (46H, m, $20XCH_2$, 6XCH), 0.687 (3H, s, tertiary CH_3), 1.064 (3H, s, tertiary CH_3), 0.855, 0.872 (3H, d) and 0.86, 0.877 (3H, d) [$RCH(\underline{CH_3})_2$], 0.895-0.929 (6H, m, $2XCH_3$), 2.465-2.485 (2H, m, allylic H), 5.42-5.43 (1H, m, olefinic H), 4.1-4.13 (2H, t, $ArOCH_2$-), 4.85-4.89 (1H, m, -CHOCOAr), 7.0-8.27 (6H, m, ArH).

Cholesteryl 2-fluoro-4-(3'-fluoro-4'-n-undecyloxybenzoyloxy)benzoate

Yield, 88%; m.p. 107°C; $[\alpha]_D^{25}$ = 1.65° (9.7mg/ml in $CHCl_3$); ν_{max} (nujol): 2950, 1740, 1700, 1620, 1470, 1120, 1180, 1290,1250 and 1060 cm^{-1}; 6: 1.09-2.17 (44H, m, $19XCH_2$, 6XCH), 0.687 (3H, s, tertiary CH_3), 1.064 (3H, s, tertiary CH_3), 0.855, 0.872 (3H, d) and 0.86, 0.877 (3H, d) [$RCH(\underline{CH_3})_2$], 0.895-0.929 (6H, m,

2XCH_3), 2.465-2.485 (2H, m, allylic H), 5.42-5.43 (1H, m, olefinic H), 4.1-4.13 (2H, t, ArOCH_2-), 4.85-4.89 (1H, m, -CHOCOAr), 7.0-8.27 (6H, m, ArH).

Cholesteryl 2-fluoro-4-(3'-fluoro-4'-n-decyloxybenzoyloxy)benzoate

Yield, 85%; m.p. 101.0°C; $[\alpha]_D^{25}$ = 0.97° (10.28mg/ml in $CHCl_3$); ν_{max} (nujol): 2950, 1740, 1700, 1620, 1470, 1120, 1180, 1290,1250 and 1060 cm^{-1}; δ: 1.09-2.17 (42H, m, 18XCH_2, 6XCH), 0.687 (3H, s, tertiary CH_3), 1.064 (3H, s, tertiary CH_3), 0.855, 0.872 (3H, d) and 0.86, 0.877 (3H, d) [RCH($\underline{CH_3}$)$_2$], 0.895-0.929 (6H, m, 2XCH_3), 2.465-2.485 (2H, m, allylic H), 5.42-5.43 (1H, m, olefinic H), 4.1-4.13 (2H, t, ArOCH_2-), 4.85-4.89 (1H, m, -CHOCOAr), 7.0-8.27 (6H, m, ArH).

Cholesteryl 2-fluoro-4-(3'-fluoro-4'-n-nonyloxybenzoyloxy)benzoate

Yield, 86%; m.p. 115.5°C; $[\alpha]_D^{25}$ = 0.91° (9.9mg/ml in $CHCl_3$); ν_{max} (nujol): 2950, 1740, 1700, 1620, 1470, 1120, 1180, 1290,1250 and 1060 cm^{-1}; δ: 1.09-2.17 (40H, m, 17XCH_2, 6XCH), 0.687 (3H, s, tertiary CH_3), 1.064 (3H, s, tertiary CH_3), 0.855, 0.872 (3H, d) and 0.86, 0.877 (3H, d) [RCH($\underline{CH_3}$)$_2$], 0.895-0.929 (6H, m, 2XCH_3), 2.465-2.485 (2H, m, allylic H), 5.42-5.43 (1H, m, olefinic H), 4.1-4.13 (2H, t, ArOCH_2-), 4.85-4.89 (1H, m, -CHOCOAr), 7.0-8.27 (6H, m, ArH).

Cholesteryl 2-fluoro-4-(3'-fluoro-4'-n-octyloxybenzoyloxy)benzoate

Yield, 87%; m.p. 115.0°C; $[\alpha]_D^{25}$ = 0.21° (14mg/ml in $CHCl_3$); ν_{max} (nujol): 2950, 1740, 1700, 1620, 1470, 1120, 1180, 1290,1250 and 1060 cm^{-1}; δ: 1.09-2.17 (38H, m, 16XCH_2, 6XCH), 0.687 (3H, s, tertiary CH_3), 1.064 (3H, s, tertiary CH_3), 0.855, 0.872 (3H, d) and 0.86, 0.877 (3H, d) [RCH($\underline{CH_3}$)$_2$], 0.895-0.929 (6H, m, 2XCH_3), 2.465-2.485 (2H, m, allylic H), 5.42-5.43 (1H, m, olefinic H), 4.1-4.13 (2H, t, ArOCH_2-), 4.85-4.89 (1H, m, -CHOCOAr), 7.0-8.27 (6H, m, ArH).

Cholesteryl 2-fluoro-4-(3'-fluoro-4'-n-heptyloxybenzoyloxy)benzoate

Yield, 90%; m.p. 141.0°C; $[\alpha]_D^{25}$ = 0.97° (10.36mg/ml in $CHCl_3$); ν_{max} (nujol): 2950, 1740, 1700, 1620, 1470, 1120, 1180, 1290,1250 and 1060 cm^{-1}; δ: 1.09-2.17

(36H, m, 15XCH_2, 6XCH), 0.687 (3H, s, tertiary CH_3), 1.064 (3H, s, tertiary CH_3), 0.855, 0.872 (3H, d) and 0.86, 0.877 (3H, d) [RCH($\underline{CH_3}$)$_2$], 0.895-0.929 (6H, m, 2XCH_3), 2.465-2.485 (2H, m, allylic H), 5.42-5.43 (1H, m, olefinic H), 4.1-4.13 (2H, t, ArOCH_2-), 4.85-4.89 (1H, m, -CHOCOAr), 7.0-8.27 (6H, m, ArH).

Cholesteryl 2-fluoro-4-(2'-fluoro-4'-n-hexadecyloxybenzoyloxy)benzoate

Yield, 85%; m.p. 90.0'~; $[\alpha]_D^{25}$ = 0.44' (11.5mg/ml in $CHCl_3$); ν_{max} (nujol): 2900, 1730, 1700, 1620, 1460, 1240, 1120 and 1020 cm^{-1}; 6: 1.08-2.16 (54H, m, 24XCH_2, 6XCH), 0.687 (3H, s, tertiary CH_3), 1.063 (3H, s, tertiary CH_3), 0.855, 0.871 (3H, d) and 0.859, 0.876 (3H, d) [RCH($\underline{CH_3}$)$_2$], 0.893-0.92 (6H, m, 2XCH_3), 2.465-2.485 (2H, m, allylic H), 5.428 (1H, m, olefinic H), 4.0-4.03 (2H, t, ArOCH_2-), 4.8-4.92 (1H, m, -CHOCOAr), 6.6-8.0 (6H, m, ArH).

Cholesteryl 2-fluoro-4-(3'-chloro-4'-n-hexadecyloxybenzoyloxy)benzoate

Yield, 80%; m.p. 113°C; $[\alpha]_D^{25}$ = 0.6' (11.5mg/ml in $CHCl_3$); ν_{max} (nujol): 2900, 1740, 1720, 1620, 1460, 1240, 1270, 1120 and 1070 cm^{-1}; 6: 1.09-2.16 (54H, m, 24XCH_2, 6XCH), 0.688 (3H, s, tertiary CH_3), 1.064 (3H, s, tertiary CH_3), 0.855, 0.872 (3H, d) and 0.86, 0.876 (3H, d) [RCH($\underline{CH_3}$)$_2$], 0.893-0.93 (6H, m, 2XCH_3), 2.46-2.48 (2H, m, allylic H), 5.43 (1H, m, olefinic H), 4.1-4.14 (2H, t, ArOCH_2-), 4.869 (1H, m, -CHOCOAr), 6.9-8.1 (6H, m, ArH).

Cholesteryl 4-(4'-n-octadecylbenzoyloxy)benzoate

Yield, 80.5%; m.p. 99.0'~; $[\alpha]_D^{25}$ = 1.09° (10.98mg/ml in $CHCl_3$); ν_{max} (nujol): 2950, 1720, 1700, 1600, 1460, 1260, 1200, 1140 and 1060 cm^{-1}; 6: 1.09-2.01 (58H, m, 26XCH_2, 6XCH), 0.688 (3H, s, tertiary CH_3), 1.06 (3H, s, tertiary CH_3), 0.855, 0.87 (3H, d) and 0.859, 0.875 (3H, d) [RCH($\underline{CH_3}$)$_2$], 0.89-0.93 (6H, m, 2XCH_3), 2.45-2.47 (2H, m, allylic H), 5.43 (1H, m, olefinic H), 2.67-2.69 (2H, t, ArCH_2-), 4.86-5.0 (1H, m, -CHOCOAr), 7.2-8.1 (8H, m, ArH).

Cholesteryl 4-(4'-n-hexadecylbenzoyloxy)benzoate

Yield, 81.5%; m.p. 112.0°C; $[\alpha]_D^{25}$ = 1.56° (12.8/ml in $CHCl_3$); ν_{max} (nujol): 2950, 1720, 1700, 1600, 1460, 1260, 1200, 1140 and 1060 cm^{-1}; 6: 1.09-2.01 (54H, m, 24XCH_2, 6XCH), 0.688 (3H, s, tertiary CH_3), 1.06 (3H, s, tertiary CH_3), 0.855, 0.87 (3H, d) and 0.859, 0.875 (3H, d) [RCH($\underline{CH_3}$)$_2$], 0.89-0.93 (6H, m, 2XCH_3), 2.45-2.47 (2H, m, allylic H), 5.43 (1H, m, olefinic H), 2.67-2.69 (2H, t, ArCH_2-), 4.86-5.0 (1H, m, -CHOCOAr), 7.2-8.1 (8H, m, ArH).

Cholestanyl 2-fluoro-4-(4'-n-octadecyloxybenzoyloxy)benzoate

This was prepared by esterifying compound 3.36 with 4-n-octadecyloxybenzoic acid using a procedure described for compound 3.31. Yield, 80%; m.p. 91.5°C; $[\alpha]_D^{25}$ = 6.8' (10.8mg/ml in $CHCl_3$); ν_{max} (nujol): 2950, 1740, 1700, 1620, 1460, 1240, 1130 and 1060 cm^{-1}; 6: 0.99-2.0 (66H, m, 28XCH_2, 7XCH, 1XCH_3), 0.65 (3H, s, tertiary CH_3), 0.85, 0.86 (3H, d) and 0.855, 0.866 (3H, d) [RCH($\underline{CH_3}$)$_2$], 0.89-0.99 (6H, m, 2XCH_3), 4.02-4.05 (2H, t, ArOCH_2), 4.93-4.98 (1H, m, -CHOCOAr), 6.95-8.1 (7H, m, ArH).

Cholestanyl 2-fluoro-4-(4'-n-octadecylbenzoyloxy)benzoate

Yield, 85%; m.p. 81°C; $[\alpha]_D^{25}$ = 6.46' (11.3mg/ml in $CHCl_3$); ν_{max} (nujol): 2950, 1740, 1710, 1620, 1470, 1260, 1130 and 1070 cm^{-1}; 6: 1.0-1.98 (66H, m, 28XCH_2, 7XCH, 1XCH_3), 0.65 (3H, s, tertiary CH_3), 0.851, 0.867 (3H, d) and 0.856, 0.872 (3H, d) [RCH($\underline{CH_3}$)$_2$], 0.89-0.99 (6H, m, 2XCH_3), 2.67-2.71 (2H, t, ArCH_2), 4.96 (1H, m, -CHOCOAr), 7.0-8.0 (7H, m, ArH).

[S]-[+]-1-Methylheptyl-4'-benzyloxybiphenyl-4-carboxylate, (3.37)

This was prepared following a esterification procedure described for compound 3.31. Thus, a mixture of 4'-benzyloxybiphenyl-4-carboxylic acid (0.75g, 2.46mmol) [55], [S]-[+]-octan-2-ol (0.35g, 2.71mmol), DMAP (0.03g, 0.24mmol) and dry dichloromethane (10ml) was stirred for five minutes. To this mixture, was added DCC (0.56g, 2.71mmol) and stirring continued overnight at room temperature. The

precipitated N,N'–dicyclohexylurea was filtered off and the filtrate diluted with dichloromethane (5ml). The resultant solution was washed with 5% aqueous acetic acid (2X5ml), water (3X10ml) and dried (Na_2SO_4). The solvent was removed from the filtered solution to yield a residue which was purified by column chromatography on silica gel using chloroform:petroleum ether (3:1) as eluent to yield pure [S]-[+]-1-methylheptyl-4'-benzyloxybiphenyl-4-carboxlate as a white solid (0.816g, 80%), m.p. 105.5°C; $[\alpha]_D^{25}$ = 46' (1mg/ml in $CHCl_3$); ν_{max} (nujol): 2950, 1700, 1600, 1460, 1380, 1270, 1290, and 1110 cm^{-1}; 6: 1.21-1.72 (10H, m, $5XCH_2$); 0.78-0.82 (6H, t, $2XCH_3$); 5.05-5.13 (3H, m, $1XCH$, $1XCH_2$); 6.98-8.0 (13H, m, ArH).
Elemental analysis: Found, C, 80.69; H, 7.73% $C_{28}H_{32}O_3$ requires C, 80.73; H, 7.74%

[S]-[+]-1-Methylheptyl-4'-hydroxybiphenyl-4-carboxylate, (3.38)

This was prepared following a procedure described for compound 3.32. Thus a mixture of [S]-[+]-1-methylheptyl-4'-benzyloxybiphenyl-4-carboxylate (0.45g, 1.1mmol) dissolved in 1,4-dioxane (10ml) and 5% Pd-C catalyst (0.11g) was stirred in an atmosphere of hydrogen at room temperature till the calculated quantity of hydrogen was absorbed. The reaction mixture was then filtered and removal of solvent under reduced pressure yielded a white solid, which was, crystallized from petroleum ether (0.315g, 88.5%); m.p. 86.5-88.5°C (Reported [56] m.p. 87-89°C); $[\alpha]_D^{25}$ = 29' (1mg/ml in $CHCl_3$); ν_{max} (nujol): 3350, 2960, 1730, 1690, 1600, 1460, 1380, 1270, 1290, and 1110 cm^{-1}; 6: 1.42-2.2 (10H, m, $5XCH_2$); 0.98-1.02 (6H, t, $2XCH_3$); 5.2-5.4 (1H, m, $1XCH$); 3.05 (1H, s, ArOH); 7.08-8.19 (8H, m, ArH).
Elemental analysis: Found, C, 77.10; H, 8.06% $C_{21}H_{26}O_3$ requires C, 77.26; H, 8.02%

[S]-[+]-1-Methylheptyl-4'-(2"-fluoro-4"-benzyloxybenzoyloxy)biphenyl-4-carboxylate, (3.39)

This was prepared following a procedure described for compound 3.37. Yield, 81.3%; m.p. 103.8°C; $[\alpha]_D^{25}$ = 29.7° (1.18mg/ml in $CHCl_3$); ν_{max} (nujol): 2950, 1720, 1735, 1600, 1460, 1380, 1260, 1290, 1140 and 1070 cm^{-1}; 6: 1.22-1.72 (10H,

m, 5XCH$_2$); 0.79-0.82 (6H, t, 2XCH$_3$); 5.08-5.14 (3H, m, 1XCH, 1XCH$_2$); 6.7-8.05 (16H, m, ArH).

[S]-[+]-1-Methylheptyl-4'-(2"-fluoro-4"-hydroxybenzoyloxy)biphenyl-4-carboxylate, (3.40)

This was prepared following a procedure described for compound 3.38. Yield, 88%; m.p. 163.0°C; $[\alpha]_D^{25}$ = 22.03' (1.18mg/ml in acetone); ν_{max} (nujol): 3400, 2950, 1720, 1620, 1470, 1280, 1140 and 1070 cm^{-1}; δ: 1.3-2.2 (10H, m, 5XCH$_2$); 0.86-0.9 (6H, t, 2XCH$_3$); 5.1-5.2 (1H, m, IXCH); 2.91 (1H, s, ArOH); 6.7-8.15 (11H, m, ArH).

[S]-[+]-1-Methylheptyl-4'-(2"-fluoro-4"-[4'"-octadecylbenzoyloxy]benzoyloxy) biphenyl-4-carboxylate, (3.41)

Yield, 89.3%; m.p. 69.0°C; $[\alpha]_D^{25}$ = 11.6' (1.2mg/ml in CHCl$_3$); ν (nujol): 2950, 1710, 1720, 1620, 1470, 1380, 1280, 1260, 1120 and 1060 cm^{-1}; δ: 0.86-1.77 (51H, m, 21XCH$_2$, 3XCH$_3$); 5.1-5.2 (1H, m, IXCH); 2.69-2.73 (2H, t, ArCH$_2$); 7.1-8.2 (15H, m, ArH).

[S]-[+]-1-Methylheptyl-4-(4"-benzyloxybiphenyl-4'-carbonoyloxy)-2-fluoro benzoate, (3.42)

This was prepared following a procedure described for compound 3.37. Yield, 78%; m.p. 139.0°C; $[\alpha]_D^{25}$ = 17.1° (2.2mg/ml in CHCl$_3$); ν (nujol): 2950, 1720, 1730, 1600, 1460, 1380, 1250, 1280, 1140 and 1070 cm^{-1}; δ: 1.20-1.70 (10H, m, 5XCH$_2$); 0.79-0.83 (6H, t, 2XCH$_3$); 5.07-5.13 (3H, m, IXCH, 1XCH$_2$); 7.0-8.1 (16H, m, ArH).

[S]-[+]-1-Methylheptyl-4-(4"-hydroxybiphenyl-4'-carbonoyloxy)-2-fluoro benzoate, (3.43)

This was prepared following a procedure described for compound 3.38. Yield, 89%; m.p. 124-126°C; $[\alpha]_D^{25}$ = 17.24' (1.16mg/ml in acetone); ν_{max} (nujol): 3400, 2900, 1710, 1740, 1600, 1460, 1240, 1280, 1140 and 1060 cm^{-1}; *6:* 1.4-2.2 (10H, m, $5XCH_2$); 1.0-1.02 (6H, t, $2XCH_3$); 5.2-5.3 (1H, m, 1XCH); 3.0-3.1 (1H, s, ArOH); 7.1-8.3 (11H, m, ArH).

[S]-[+]-1-Methylheptyl-4-(4"-[3"'-fluoro-4"'-n-hexadecyloxybenzoyloxy] biphenyl-4'-carbonoyloxy)-2-fluorobenzoate

Yield, 85%; m.p. 79.0°C; $[\alpha]_D^{25}$ = 8.9' (1.46mg/ml in $CHCl_3$); ν_{max} (nujol): 2900, 1710, 1720, 1600, 1450, 1340, 1380, 1280, 1260, 1120 and 1060 cm^{-1}; δ: 0.86-1.91 (47H, m, $19XCH_2$, $3XCH_3$); 5.15-5.2 (1H, m, 1XCH); 4.1-4.14 (2H, t, $ArOCH_2$); 7.0-8.27 (15H, m, ArH).

REFERENCES

[1] F.Reinitzer, Monatsh. Chem., 9,421 (1888).

[2] O.Lehmann, *Z.* Phys. Chem., 4,462 (1889).

[3] D.Coates and G.W.Gray, Phys. Lett., **45A**, 115 (1973).

[4] D.W.Berreman, Liquid Crystals and Ordered Fluids, Plenum Press, New York, 4,925 (1984).

[5] R.B.Meyer, *Mol. Cryst.* Liq. *Cryst.*, **40**, 33 (1977).

[6] R.B.Meyer, L.Leibert, L. Strzelecki and P.Keller, Phys. Lett., **36**, 69 (1976).

[7] J.W.Goodby, M.A.Waugh, S.M.Stein, E.Chin, R.Pindak and J.S.Patel, Nature, London, 337,449 (1989).

[8] P.G.de Gennes, Solid State Commun., 10,753, (1972).

[9] S.R.Renn and T.C.Lubensky, Phys. Rev. A., 38,2132 (1988).

[10] J.W.Goodby, M.A.Waugh, S.M.Stein, E.Chin, R.Pindak and J.S.Patel, J. Am. Chem. *Soc.*, 111,8119 (1989).

[1I] A.J.Slaney and J.W.Goodby, *J.* Mater. Chem., 1, 5 (1991).

[12] A.J. Slaney, *PhD* Thesis, University of Hull (1992).

[13] J.W.Goodby, I.Nishiyama, A.J.Slaney, C.J.Booth and K.J.Toyne, Liq. *Cryst.*, **14**, 37 (1993).

[14] J.W.Goodby, I.Nishiyama, A.J.Slaney, J.Vuijk, C.J.Booth, P.Styring and P.Toyne, Mol. *Cryst.* Liq. *Cryst.*, 243,231 (1994).

[15] H.T.Nguyen, A.Bouchta, L.Navailles, P.Barois, N.Isaert, R.J.Tweig, A.Maaroufi and C.Destrade, J. Phys II. France., 2, 1889 (1992).

[16] A.Bouchta, H.T.Nguyen, M.F.Archard, F.Hardouin, C.Destrade, R.J.Tweig, A.Maaroufi and N.Isaert, Liq. *Cryst.*, 12,575 (1992).

[17] M.H.Li, V.Laux, H.T.Nguyen, G.Gigaud, P.Barois and N.Isaert, Liq. *Cryst.*, 23, 389 (1997).

[18] R.Shao, J.Pang, N.A.Clark, J.A.Rego and D.M.Walba, Ferroelectrics, 147, 255 (1993).

[19] A.J.Slaney and J.W.Goodby, J. Mater. Chem., 5,663 (1995).

[20] W.J.Hsieh and S.L.Wu, *Mol. Cryst.* Liq. *Cryst.*, 302, 253 (1997).

[21] (a) L.Navailles, H.T.Nguyen, P.Barois, C.Destrade and N.Isaert, Liq. *Cryst.*, 15, 479 (1993). (b) H.T.Nguyen, A.Babeau, J.C.Rouillon, G.Sigaud, N.Isaert and F.Bougrioua, Ferroelectrics, 179, 33 (1996).

[22] P.Balkwill, D.Bishop, A.Pearson and I.Sage, Mol. *Cryst.* Liq. *Cryst.*, 123, 1 (1985).

[23] V.Reiffenrath, J.Krause, H.J.Plach and G.Weber, Liq. *Cryst.*, 5, 159 (1989).

[24] M.A.Osman, Mol. *Cryst.* Liq. *Cryst.*, **128**, 45 (1985).

[25] C.Viney, R.J.Twieg, T.P.Russell and L.E.Depero, Liq. *Cryst.*, 5, 1793 (1989).

[26] H.T.Nguyen, C.Destrade, J.P.Parneix, P.Pochat, N.Isaert and C.Girold, Ferroelectrics, 147, 181 (1993).

[27] J.I.Jin, H.S.Kim, J.W.Shin, B.Y.Chung and B.W.Jo, Bull. Korea Chem. *Soc.*, 11,209 (1990).

[28] F.Hardouin, M.F.Archard, J.I.Jin, J.W.Shin and Y.K.Yun, J. Phys II. France., 4, 627 (1994).

[29] Y.S.Freidxon, Y.G.Tropsha, V.V.Tsukruk, V.V.Shilov, V.P.Shibaev and Y.S.Lipatov, J. Polym. Chem., 29,1371 (1987).

[30] Y.Sah, Mol. *Cryst.* Liq. *Cryst.*, 302,207 (1997).

[31] G.W.Gray, C.Hogg and D.Lacey, Mol. *Cryst.* Liq. *Cryst.*, 67, 1 (1981).

[32] D.Demus and L.Richter, Textures Of Liquid *Crystals*,Weinheim, New York (1978).

[33] V.Vill, J.Thiem, Z. *Naturforsch.*, 450, 1205 (1990).

[34] R.M.Cherkashina, L.A.Kutulya, A.V.Tolmachev and V.G.Tishchenko, Zh. Obshch. Khim., 56,454 (1986).

[35] L.A.Kutulya, R.M.Cherkashina, T.V.Khandrimailova, V.G.Tishchenko, A.P.Shkumat, V.E.Kuzmin and L.P.Trigub, Zh. Obshch. Khim., 56,462 (1986).

[36] P.M.Agocs, G.Motika, J.A.Szabo and A.I.Zoltai, *Acta.* Phys. Chem., 25, 173 (1979).

[37] P.J.Collings, T.J.McKee and J.R.McColl, J. Chem. Phys., 65, 3520 (1976).

[38] J.W. Sanders, *PhD* Thesis, Kent (1969).

[39] A.A.Gerasimov, Ukr. Fiz. Zh., 33, 1177 (1988).

[40] L.A.Kutulya, R.M.Cherkashina, V.G.Tishchenko and T.V.Khandrimailova, Zhidk. Kristally., Ivanovo, 100 (1985).

[41] H.T.Nguyen, R.J.Twieg, M.F.Nabor, N.Isaert and C.Destrade, Ferroelectrics, 121, 187 (1991).

[42] P.G.de Gennes and J.Prost, The Physics Of Liquid Crystals, 2'' ed., Clarendon Press, Oxford (1993).

[43] S.R.Renn and T.C.Lubensky, *Mol. Cryst.* Liq. *Cryst.*, 209,349 (1991).

[44] S.R.Renn, Phys. Rev. A., 45,953 (1992).

[45] N.Isaert, L.Navailles, P.Barois and H.T.Nguyen, J. Phys. II France., 4, 1501 (1994).

[46] L.Navailles, R.Pindak, P.Barois and H.T.Nguyen, Phys. Rev. Lett., 74, 5224 (1995).

[47] P.A.Pramod, R.Pratibha and N.V.Madhusudana, Current Science, 73, 761 (1997).

[48] G.W.Gray and B.Jones, J. Chem. *Soc*., 4179 (1953).

[49] C.Weigand and R.Gabler, *Z.* Phys. Chem., **B46**, 270 (1940).

[50] S.A.Langer and J.P.Sethna, Phys. Rev. A., 34,5035 (1986).

[51] G.A.Hinshaw and R.G.Petschek, Phys. Rev. A., 39,5914 (1989).

[52] G.A.Hinshaw and R.G.Petschek, Phys. Rev. Lett., 60, 1864 (1988).

[53] E.Górecka, M.Glogarová, H.Sverenyák and L.Lejček, *Ferroelectrics*, 178, 101 (1996).

[54] A.Hassner and V.Alexanian, Tetrahedron Lett., 4475 (1978).

[55] N.Kasthuraiah, *PhD* Thesis, Bangalore University, India (1997).

[56] C.J.Booth, D.A.Dunmur, J.W.Goodby, J.S.Kang and K.J.Toyne, J. *Mater.* Chem., 4,747 (1993).